

PINE SEEDLING DETECTION AND REGISTRATION

Except where reference is made to the work of others, the work described in this thesis is my own or was done in collaboration with my advisory committee. This thesis does not include proprietary or classified information.

Jeffrey K. Hunt

Certificate of Approval:

John Y. Hung, Co-Chair
Professor
Electrical and Computer Engineering

Timothy P. McDonald, Co-Chair
Associate Professor
Biosystems Engineering

Thomas Baginski
Professor
Electrical and Computer Engineering

John P. Fulton
Assistant Professor
Biosystems Engineering

George T. Flowers
Dean
Graduate School

PINE SEEDLING DETECTION AND REGISTRATION

Jeffrey K. Hunt

A Thesis

Submitted to

the Graduate Faculty of

Auburn University

in Partial Fulfillment of the

Requirements for the

Degree of

Master of Science

Auburn, Alabama
December 18, 2009

PINE SEEDLING DETECTION AND REGISTRATION

Jeffrey K. Hunt

Permission is granted to Auburn University to make copies of this thesis at its discretion, upon the request of individuals or institutions and at their expense. The author reserves all publication rights.

Signature of Author

Date of Graduation

VITA

Jeffrey Hunt, son of Raymond Hunt and Teresa Surrey, was born February 26, 1985, in Mobile, Alabama. He graduated from Robertsdale High School in 2003. He attended Auburn University in September 2003 and graduated with a Bachelor of Electrical Engineering degree in May 2007. He enrolled in Graduate School at Auburn University, June 2007. He worked as a graduate teaching assistant for the Department of Electrical Engineering and as a research assistant for the Department of Biosystems Engineering. He graduated December 2009 with a Master's of Science in Electrical Engineering.

THESIS ABSTRACT
PINE SEEDLING DETECTION AND REGISTRATION

Jeffrey K. Hunt

Master of Science, December 18, 2009
(B.S., Auburn University, 2007)

91 Typed Pages

Directed by John Y. Hung and Timothy P. McDonald

Pine seedling nurseries across the United States depend on antiquated techniques and equipment to manage the country's supply of pine seedling stock. This research is directed towards the development of a method to autonomously inventory and manage pine seedlings while in the nursery bed. Several electronic technologies are analyzed and compared to determine their performance as a pine seedling detection and registration sensor for nurseries. The technologies of interests are: photo-interrupt sensors, capacitive sensors, microwave sensors, computer vision, and radar. A key component in determining which technology to pursue was its ability to obtain an accurate inventory with low processing cost. The ability to determine the overall health of the pine seedlings was also an important consideration. The final goal of this research is to catalog each technologies performance as a pine seedling detection and registration sensor for the future development of an auto-indexing pine seedling counter.

ACKNOWLEDGMENTS

This thesis would not have been possible without the support and dedicated faculty found at both the Department of Electrical Engineering and the Department of Biosystems Engineering. A special thanks goes to each of my advisers. Dr. Hung, thank you for providing focus during the extent of the research process. Dr. McDonald, thank you for your direction and constant support. Dr. Baginski, thank you for your willingness to think outside the box and try new ideas. Dr. Fulton, thank you for editing and your words of encouragement. I would also like to recognize Dr. Riggs for his extensive assistance. His knowledge in the area of electromagnetics was true north for this research.

Style manual or journal used Journal of Approximation Theory (together with the style known as “aums”). Bibliography follows van Leunen’s *A Handbook for Scholars*.

Computer software used The document preparation package T_EX (specifically L^AT_EX) together with the departmental style-file `aums.sty`.

CONTENTS

LIST OF FIGURES	x
1 INTRODUCTION	1
1.1 Motivation	1
1.2 Current Method	1
1.3 Research Value	2
1.4 Previous Work	3
1.5 Approach	4
1.5.1 Method Specifications	5
1.6 Objectives	6
2 CURRENT INVENTORY MANAGEMENT TECHNOLOGIES	7
2.1 Photo-Interrupt Sensing	7
2.2 Capacitive Sensing	8
2.3 Microwave Sensing	9
2.4 Object Registration via Computer Vision	10
2.5 Object Registration via Radar	10
2.6 Summary	11
3 RESEARCH PROCEDURES	12
3.1 Introduction	12
3.2 Photo-Interrupt Detection Experiment	12
3.3 Capacitive Sensing Experiment	14
3.4 Computer Vision Experiment	15
3.5 Radar Experiments	17
3.5.1 Radar Return Signal Measurement	17
3.5.2 Radar Backscatter Measurement	17
4 RESULTS AND DISCUSSION	23
4.1 Photo-Interrupt Results	23
4.2 Capacitance Sensor Results	24
4.3 Computer Vision Results	25
4.4 Radar Results	30
4.4.1 Monopole Tree Model	30
4.4.2 Ideal Loblolly Model	33
4.4.3 Sample Seedling Model	35

5	SUMMARY AND CONCLUSIONS	37
5.1	Introduction	37
5.2	Future Work	39
	BIBLIOGRAPHY	41
	APPENDICES	43
A	PHOTO-INTERRUPT MICROCONTROLLER SCHEMATIC	44
B	PHOTO-INTERRUPT MICROCONTROLLER CODE	45
C	CAPACITIVE SENSOR SCHEMATIC	58
D	CAPACITIVE SENSOR MATLAB CODE	59
E	CAPACITIVE SENSOR COLLECTED DATA	61
F	MATLAB CODE FOR IMAGE PROCESSING	74
G	NEC WIN-PRO CODE FOR PINE SEEDLING MODELS	76
H	SIMULATED RADAR RETURN DATA	78

LIST OF FIGURES

3.1	Typical Pine Seedling Nursery Bed [2]	12
3.2	Artificial Pine Seedling Test Bed	13
3.3	Photo-Interrupt Experiment Setup	14
3.4	Capacitive Experiment	16
3.5	Incident Plane Wave Referenced to the Model	18
3.6	Ideal Loblolly Pine & Sample Pine Seedling [21]	19
3.7	NEC Win-Pro Wire Models	20
3.8	Sampled Dielectric Loads	22
4.1	Seedling Position and Measured and Modeled Capacitance	24
4.2	Seedling Harvester Infra-Red Guidance Camera	25
4.3	Infra-Red Photographs of Artificially Spaced Pine Seedlings	26
4.4	Ultra-Violet Photographs of Artificially Spaced Pine Seedlings	26
4.5	Plant Absorption of Light in the Visible Spectrum [14]	27
4.7	Series of Images with Data Vector	29
4.6	Visible Spectrum Analysis	29
4.8	Voltage Waveform Induced from the Current Flow through a Pine Seedling due to the presence of an Electromagnetic Field	31
4.9	Radiation Pattern of the Monopole Tree Model	32
4.10	Monopole Antenna Reradiated Power	33
4.11	Radiation Pattern of Ideal Loblolly Model	34

4.12	Loblolly Antenna Re-radiated Power	34
4.13	Radiation Pattern of the Sample Seedling Model	35
4.14	Sample Seedling Antenna Re-radiated Power	36
A.1	Photo-Interrupt Microcontroller Schematic	44
C.1	Capacitive Sensor (Cx represents electrodes)	58

CHAPTER 1
INTRODUCTION

1.1 Motivation

The production of pine seedlings for the purpose of reforestation is a crucial part of sustaining the earth's forests. Pine seedlings and other tree seedlings are grown and purchased every year to reforest millions of acres of timberlands. The timber industry is the largest producer and purchaser of pine seedlings for reforestation. The timber company Weyerhaeuser produces the most annually in the United States at over 20 million seedlings a year just for their own timberlands [4]. Seedlings grown for reforestation in the United States are mainly a variety of pine seedlings.

Pine seedling nurseries across the United States depend on antiquated techniques and equipment to manage the countries supply of pine seedling stock. The high volume of pine seedlings produced each year combined with the limited amount of nursery land has pushed nurseries to become more efficient in production and inventory management. Nursery managers are already pushing the limits of production by increasing the number of seedlings planted per square foot to the maximum viable limits [20]. Interest in creating a more efficient process has generated research into the development of a better inventory management system.

1.2 Current Method

Generating an accurate count of the number of seedlings in a field is the main concern presented by nursery managers. Currently there is no standard method or system in place to inventory seedlings in the field or during harvest. The method commonly used for obtaining a seedling count prior to harvesting is to count the number of seedlings, manually, in a

predetermined section of a row. The number of seedlings counted is divided by the row length yielding a count-length. The count-length is considered the average number of trees found in a unit length of row. Nursery managers then use the count-length to estimate the overall inventory for the field and as a guide to determine how much of a row must be harvested to fill an order.

Nursery managers would also like to maintain a count of seedlings during the harvesting process. Seedling orders arrive at the nursery and an estimation is made out in the field as to how much of the seedling bed to harvest to fill the order using the count-length method. The seedlings are pulled from the nursery bed with a harvester and taken to a shed for processing. The current method for counting seedlings post harvest is to count, by hand, a sub-sample. The sub-sample is then weighed and a count-weight is established. A count-weight is the weight of a pre-established number of trees, in most cases the number is 50 or 100. Groups of seedlings are weighed and bundled according to their weight and grade. A seedling's weight is mainly a function of its moisture content, which changes dynamically from one batch to the next. The count-weight is updated constantly to average dynamic changes in moisture for a more accurate count. The count-weight method is the current inventory process for most pine seedling nurseries in the Southeastern part of the United States.

Both methods are inaccurate, so the nursery managers must ensure generous portions of tree stock for the consumer, which cuts into the efficiency of the nursery operation. Although automated inventory systems have been developed in the past, none are currently in use due to their poor performance.

1.3 Research Value

Managers are primarily in need of a automated system to obtain an accurate count of pine seedlings in the field. The development of a pine seedling detection and registration system would be beneficial to the entire nursery operation. The value of this research is to provide nursery managers with a modern tool to inventory more efficiently. Nursery

managers could maintain better quality control by making proper irrigation and fertilization adjustments according to seedling density plots. A system capable of grading seedlings would increase the efficiency of the operation by identifying seedling rows ready for harvest. Grading the seedlings in the field would reduce the time to package. The field inventory would also ensure that the proper quantity of seedlings are harvested and packaged. Developing an automated system will provide nursery manager's with a tool to better control the efficiency and the quality of the entire inventory process.

1.4 Previous Work

A system for auto-indexing seedlings was patented in 1977 by an inventor, Rath [3]. Rath designed a harvester he claimed was capable of counting, grading, and bundling seedlings as they were lifted from the nursery bed. His invention used a photo-interrupt sensor to count and grade seedlings, but it was never adopted by the seedling industry.

The United States government has funded research for a device to count seedlings. In 1991 a seedling counter was developed by the USDA Forest Service's Missoula Technology and Development Center (MTDC) in cooperation with Dr. Glenn Kranzler of Oklahoma State University. The device was built to count a single row of conifer seedlings in a nursery bed. Their objective was to automate the inventory process. The outcome was a custom-designed photo-interrupt system controlled by a portable computer which could count a single row of seedlings with rows spaced at least 6 inches apart. The seedlings were required to be at least .08 inches (2mm) in diameter and 2 inches (5.1 cm) in height to be counted. Due to the large number of seedlings in a nursery it was suggested that the gross inventory could be estimated based on the count obtained from one row¹. The results of this study were disappointing, often recording between 70-90% of the total number of seedlings in a row. The study recommended that a precision seeder would improve the accuracy by evenly spacing the seedlings [1]. Several other explanations were given to account for the counter's

¹This method is similar to the count-length method previously described in the current method section.

inaccuracy, such as mounds that occur at the root collar of the seedlings due to the effects of irrigation, false interrupts from branches, and false interrupts from foliage density.

Other types of tree registration technologies have been developed from radar and Li-DAR² for applications in forestry management [5]. Researchers have been interested in developing a way to monitor and map forests on a global scale to ensure sustainable forestry. Several techniques have developed from this interest and most of those techniques make use of two technologies: Li-DAR³ and InSAR⁴. Li-DAR is typically used to obtain stand heights from an airborne system. The system's airborne Li-DAR sensor scans the ground to obtain the aircraft to ground distance and the aircraft to tree crown distance. The differential between the two measurements provides the stand height at the scanned location.

InSAR is used to obtain characteristics that cannot be detected optically such as canopy volume and biomass. InSAR is currently being researched as a possible tool to make individual tree measurements. Researchers are suggesting that airborne InSAR data of forest stands can be used to build a two dimensional map of a forest stand. The same InSAR system could tag each tree on the map with specific information pertaining to that tree such as height and stocking volume. These technologies can potentially be applied to pine seedling detection and are examined in this thesis.[5]

1.5 Approach

An evaluation of the best applicable sensing technology is needed based on the limited amount of literature and research performed on pine seedling detection and registration. The development of a pine seedling detection and registration method will require studying several detection methods. The approach of this research is to take a broad view of current inventory management technologies and analyze each technology's strengths and weaknesses for its application in a seedling nursery. The evaluation of each technology's performance

²Light Detection and Ranging

³Light Detection and Ranging

⁴Interferometric Synthetic Aperture Radar, aka IFSAR

is based on the method specifications. The method specifications presented represent the needs of nursery managers and the limitations that exist in the nursery environment.

1.5.1 Method Specifications

During the November 7, 2007 Auburn University-Southern Forest Nursery Management Cooperative (SFNMC) Advisory Meeting, nursery management from the south eastern United States were asked to provide specifications for a proposed pine seedling sensor. The sensor would be incorporated into an inventory management and control system. The desired specifications are presented in the following subsections.

Inventory

The sensor should have the ability to inventory seedling populations during various stages of the seedling growth cycle, primarily the mid to late stages. This counting includes seedlings at variable heights and stem diameters. The sensor would need to operate in the nursery's outdoor environment, which includes but is not limited to precipitation, dust, dirt, and wind.

Real-time Harvest Count

The sensor will need to count seedlings while harvesting to prevent inventory loss due to the perishability of the product. This system requirement would demand the sensor to operate on-the-fly⁵ through a row of seedlings. A sensor mounted to the front of a tractor or possibly mounted on the harvester was proposed by one nursery manager. He also proposed that a two dimensional plot of seedling's location be established prior to harvesting, giving the harvester an accurate guide to determine how much product should be harvested.

⁵typically 1 mile per hour

Non-Invasive

The sensor system will need to remain non-invasive to protect the quality of the seedlings while in their early stages of development. A non-invasive system is also desirable during harvesting to ensure no damage or disorientation is caused to the trees on their way to and through the harvester.

Grading Capability

The final system requirement provides for an automatic grading capability giving the user an option to identify trees based on root collar diameter. An option to identify diseased trees was also proposed by Dr. Timothy McDonald.

1.6 Objectives

The need for automated pine seedling detection and registration for the better inventory management of pine seedling nurseries is the reason for conducting this research. Inventory acquisition techniques currently used by seedling nurseries are in need of modernization. A more efficient inventory process is needed to improve the productivity of pine seedling nurseries. The goals of this research will be reached by accomplishing the following objectives.

1. Review fundamental technologies for modern inventory control and management as they apply to the problem of pine seedling detection and registration.
2. Model and test each technology using a selected detection and registration method.
3. Catalog the strengths and weaknesses of each detection and registration method as it pertains to the future development of automated pine seedling detection and registration.

CHAPTER 2

CURRENT INVENTORY MANAGEMENT TECHNOLOGIES

Thousands of sensors have been developed for general inventory management and are available commercially. Most inventory sensors were developed for use in controlled environments such as libraries, factories, and warehouses. Each of those inventory sensors are based on central principles from a particular detection technology. For instance, light detection has evolved from a single detection diode to Li-DAR and computer vision which are completely different types of detection. Five basic detection principles exist for a majority of the inventory management sensors: photo-interrupt, capacitance, microwave, computer vision, and radar. These fundamental sensing techniques will be analyzed for their potential application to the problem of pine seedling detection and registration.

2.1 Photo-Interrupt Sensing

A photo-interrupt sensor consists of two components, an emitter diode and a detection diode. The emitter diode sends a beam of light directed to the detector diode or the beam is reflected to the detector diode. The detector diode receives the light-beam and sends an electrical current to a control unit. The current is non-linearly proportional to the amount of light gathered by the detector. The sensor control unit sets a detection threshold which limits the output of the sensor's controller to two states, detection or no detection of the light beam. The output of the controller is effectively a binary signal, representing the interruption of the light beam.

Photo-interrupt is commonly used in industry due to its simplicity and dependability. The sensor provides an easy way to count, maintain proper spacing, or ensure size

parameters on an assembly line. Gasvoda’s paper [1], describes the photo-interrupt system developed by MTDC. It uses multiple sensors arranged in a vertical column to detect conifer seedlings. The vertical geometry of the photo-interrupt network helps to distinguish between horizontal limbs and vertical stems. A pine seedlings stem is a good way to count a pine seedling because all pine seedlings have only one central stem. The paper states the main weakness of a photo-interrupt system is false interrupts contributed by the nursery’s environment.

2.2 Capacitive Sensing

Capacitive sensors typically consist of two electrodes and a voltage source to generate an electric field between the two electrodes. The amplitude of the source and geometry of the electrodes determines the size and shape of the generated electric field. Equation 2.1 describes the relationship between capacitance, dielectric medium, and the electrode’s geometry for a parallel plate capacitor. The capacitance C is proportional to the area of the electrodes A divided by the distance between the electrodes d multiplied by the permittivity of the dielectric medium between the plates. The sensor detects the change in the electric field when an insulator, also known as a dielectric, passes between the electrodes. The change in the electric field is dependent on the materials relative static permittivity ϵ_r . The measured characteristic of the material is also referred to as its relative dielectric constant.[6]

$$C = \epsilon_r \epsilon_0 \frac{A}{d} \tag{2.1}$$

Capacitive sensors are typically selected for their robustness and low cost. They are used in industry as position sensors, determining the distance between objects. This property allows for their use in pressure sensors by determining the distance between a fixed position and an elastic diaphragm. Capacitance sensors are also used as liquid level fill sensors and as material detection sensors. Capacitive sensors have previously been used in

agriculture as a moisture sensor for grain and other solid flow applications [14]. A capacitance sensor could possibly be configured as a material detection sensor and used to register pine seedlings by detecting their presence between two electrodes.

2.3 Microwave Sensing

Microwave sensors typically consist of a controller, a transmitting antenna, and a receiving antenna. The transmitter produces microwaves that are directed through a material of interest and into the receiver. The receiver detects the microwave signal and the controller records the phase shift and attenuation observed between the sent and received signals. The controller uses the phase shift and attenuation as parameters to measure and determine the materials dielectric permittivity. Phase shift and attenuation are dependent upon the permittivity of the medium between the transmitting and receiving antennas. Equation 2.2¹ defines phase shift and attenuation as the electric displacement field vector \hat{D} . The electric displacement field is shown as function of the electric field intensity \hat{E} produced by the transmitting antenna multiplied by a material's permittivity $\hat{\epsilon}$. [8]

$$\hat{D} = \hat{\epsilon}\hat{E} \tag{2.2}$$

Microwave sensors are commonly used in industry as moisture detection sensors. Microwave moisture sensors take advantage of water's molecular dipole structure and the effect it has on attenuating microwaves. Microwave technology has been applied to inventory management with the development of RFID² tags. The tags are uniquely coded for each type of inventoried item and are physically attached to that item. The inventory count is modified if the item, with attached RFID, passes between a transmitting and detecting antenna. Placing RFID tags on each seedling is not feasible and could possibly be invasive causing damage to the seedlings. A microwave sensor, like the capacitive sensor, could be setup for

¹Equation 2.2 is for a linear, homogeneous, and isotropic material.

²Radio Frequency Identification

material detection of pine seedlings. However the transmitting and receiving antennas must be generously spaced apart for far field operation.

2.4 Object Registration via Computer Vision

Computer vision is the youngest sensing technique and employs the use of a digital camera and light source. The light source is dependent on which spectrum is of interest, because cameras are capable of processing infrared, ultraviolet, and the visual spectrum. The sensor works by capturing the reflected light from the camera's field of view and producing a digital image of the scene. The image must then be processed by a controller to determine if any valuable data is present.

Computer vision is capable of object detection, recognition, and tracking. Object detection is of interest for its possible applications in inventory management and pine seedling registration. Object detection uses a controller to process an image based on an object identification algorithm. The algorithm's output is processed to detect if the object of interest is present. If the controller detects the object is present, then it may be able to reprocess the image and determine other optical characteristics of the object such as size. Several algorithms for object detection have been developed using computer vision such as edge detection, corner detection, cross correlation, and statistical analysis. The algorithms have possible applications to the problem of pine seedling detection and registration. [12]

2.5 Object Registration via Radar

Traditional CW³ radar consists of a controller, a transmitting antenna, and a receiving antenna. The transmitting and receiving antenna are sometimes combined into one structure. The transmitting antenna sends out a signal of a sine wave carrier modulated with narrow rectangular pulses. The signal is directed at the object of interest also known as the target. The distance from the target to the radar is determined by measuring the

³Continuous-wave

time it takes for a radar signal to travel to the target and return to the receiver, T_R . Since electromagnetic energy propagates at the speed of light c , the range R is

$$R = \frac{cT_R}{2} \tag{2.3}$$

Radar is best known for its military defense applications, however it has been used in forestry to map the earth's topography and also to monitor the condition of our planet's forests. Researchers have used radar in combination with Li-DAR to develop a more accurate map of a forest's biomass and stand heights. There is also an interest in using radar to spatially map forest stands as mentioned above in the previous work section. Radar has the ability to collect data over a large area very quickly and potentially retrieve spatial information as demonstrated in [5].

2.6 Summary

Five principle sensing technologies have been reviewed for sensing abilities. Of the five reviewed, four were selected for further research and testing. The four technologies are photo-interrupt detection, capacitive sensing, computer vision, and radar detection. Microwave sensing was omitted due to its similarity to capacitive sensing in its ability to determine the dielectric constant and its limitation to far field operation. The remaining technologies were evaluated through experimentation for their application to the pine seedling detection and registration problem.

CHAPTER 3

RESEARCH PROCEDURES

3.1 Introduction

A sample set of mature pine seedlings were donated for experimentation by a seedling nursery. The seedlings were transplanted into a large container and spaced to artificially resemble the row density found in a typical nursery bed. Figure 3.1 depicts pine seedlings in a nursery bed (left) and the density that pine seedlings are grown (right). The artificial test bed shown in Figure 3.1 was subjected to the selected sensing methods to test for their capabilities and limitations. The following experiments were conducted to provide insight into sensing technologies for a method of pine seedling detection and registration.

3.2 Photo-Interrupt Detection Experiment

A Photo-interrupt system is the logical place to start and is the only technology previously tested for pine seedling detection. An experiment was set up to resemble the



Figure 3.1: Typical Pine Seedling Nursery Bed [2]



Figure 3.2: Artificial Pine Seedling Test Bed

photo-interrupt seedling counter developed by MTDC's previous research [1]. The Banner QS18VP6LLP retro-reflective laser sensor was selected as the photo-interrupt sensor for this experiment because of its ability to operate with the emitter and detector in close proximity [18]. Another benefit of this retro-reflective sensor is the beam must be reflected back to the sensor's detector at an angle. The reflection angle provides an increase in realized beam height. Like MTDC's device, the sensor's emitter, detector, and reflector were mounted to a frame for traveling down a single row of seedlings. The beam width was selected to be 3mm, half the average diameter of the sample set of seedlings. The beam width was chosen to ensure the count of seedlings that may be under grown while screening out small vertical limbs and foliage.

A sensor controller was developed from a 16F747 PIC microcontroller. The sensor was debounced with the controller permitting a maximum count rate of 100 seedlings per second. The assembly code for the controller can be found in Appendix A. Unlike MTDC, this experiment does not use a controller to monitor a vertical array of photo-interrupts.

The vertical array allowed the system to differentiate between horizontal obstructions and vertical stems. Instead, the sensor relies on its retro-reflective structure to provide a narrow and tall beam. The final configuration gives the sensor a realized beam height of one centimeter and is shown in Figure 3.2.

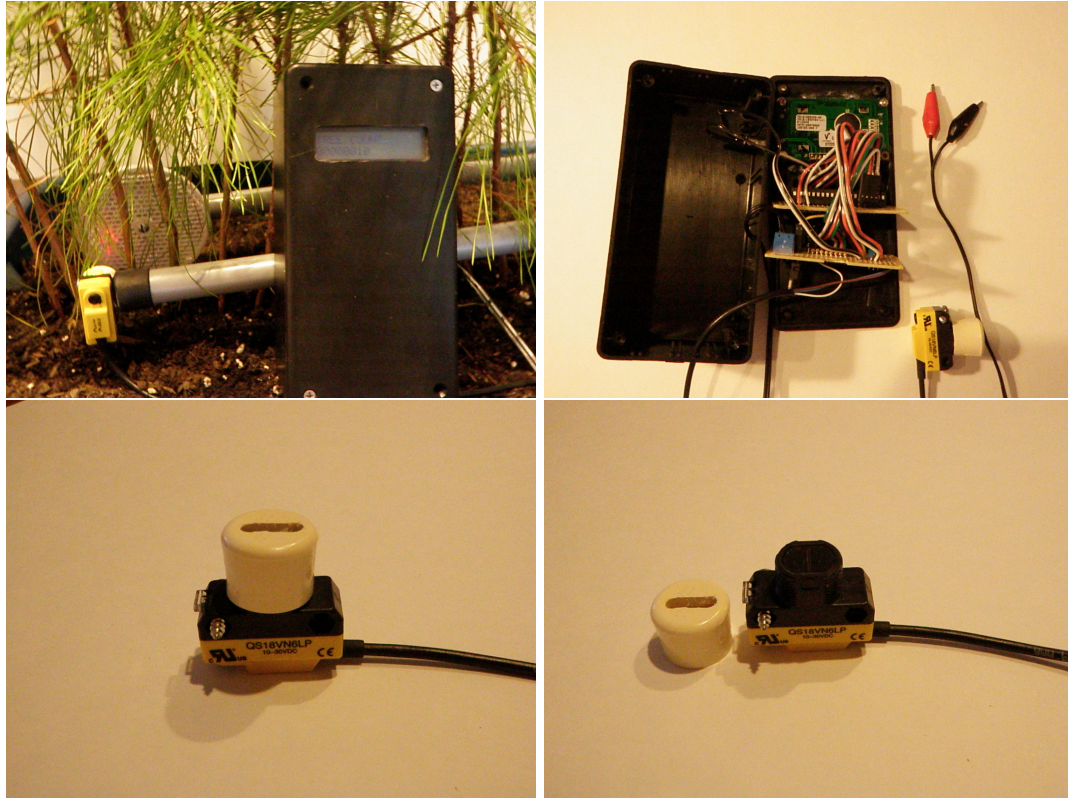


Figure 3.3: Photo-Interrupt Experiment Setup

3.3 Capacitive Sensing Experiment

Capacitive sensors effectively measure the dielectric properties of any material that passes into its electric field. Since pine seedlings are non-conductive they are considered insulators or more commonly called dielectrics. According to equation 2.1, a material's dielectric constant is proportional to its capacitance. The dielectric constant of a pine seedling can be determined by measuring the capacitance of two parallel plates with a seedling as the dielectric medium. Placing more dielectric medium between the electrodes

will increase the capacitance. A pine seedling count could be determined if capacitance is related to the number of seedlings between two electrodes.

An experiment was designed to determine if capacitance is related to the number of seedlings between two electrodes. The size of the electrodes was designed to maximize the seedling stem's effect on the electric field while maintaining a measurable capacitance. The electrodes were mounted to a frame and spaced 10 cm apart. The frame allowed sample seedlings to pass through the electric field between the electrodes. A custom capacitance measuring circuit was constructed to convert capacitance into a measurable voltage. Care was taken to shield the electrodes, sensing cables, and the custom capacitance measuring circuit. The sensor setup is shown in Figure 3.3. As the electrodes passed down the row of seedlings the sensor measured the capacitance between the electrodes and converted the capacitance into a representative voltage. The sensor's output was then measured by a digital multimeter.

3.4 Computer Vision Experiment

Computer vision uses an object's color, intensity, and shape for identification and registration. These characteristics are known about pine seedlings only in the visible spectrum. An experiment was designed to examine the set of artificially planted pine seedlings in the infrared, ultraviolet, and visible spectrum's. The goal is to reveal any potential color or intensity qualities that can be exploited to distinguish pine seedlings in an image. A Sony Handycam camera was used to take digital images of the pine seedling for image processing and analysis. The camera used the sun as a source of light and collected images from the side of one artificial pine seedling row. Sunlight was the logical source of illumination for the camera because sunlight emits infrared, visible, and ultraviolet light. Also, nurseries grow pine seedlings outdoors and nursery operations are performed during the day.



Figure 3.4: Capacitive Experiment

3.5 Radar Experiments

3.5.1 Radar Return Signal Measurement

Two experiments were developed to test radar's ability to detect pine seedlings. The first experiment tested a pine seedling's measurable radar return signal. The experiment uses a discone antenna as a signal transmitter to propagate a plane wave. The discone antenna design allows it to transmit a vertically polarized wideband signal omnidirectional. The vertical polarization of this antenna design is expected to help couple the propagated wave to the vertical stem of the pine seedling. A signal generator was used to produce a wideband signal and propagate it from the discone antenna to a sample pine seedling in the far field. The sample seedling will generate a return if it has internal current flow. A Pearson coil¹ is used to detect any internal current flow in the seedling and convert the current flow into a readable voltage on an oscilloscope. During the experiment the Pearson coil will only be coupled to the pine seedling allowing the seedling's return to be isolated from the return of other objects in the room.

3.5.2 Radar Backscatter Measurement

The second experiment tests a pine seedling's signal backscatter characteristics. The concern with using radar for pine seedling detection is radar's ability to distinguish a pine seedling from foliage. The seedlings measured backscatter will determine if the return is a function of only the seedling or if foliage contributes. The portion of backscatter that returns in the direction from which the transmitted plane wave originates is called the radar return. A radar system will need to detect a return based on each seedling's stem.

The test for radar return requires a software simulation tool to model a pine seedling's backscatter response to an electromagnetic field. Backscatter measurements are used to identify a target with a radar system. Several methods of computing radar backscatter have been developed for a variety of target geometries. The geometry of a pine seedling

¹A Pearson coil measures the induced voltage from the magnetic field generated by a change in current through the coil

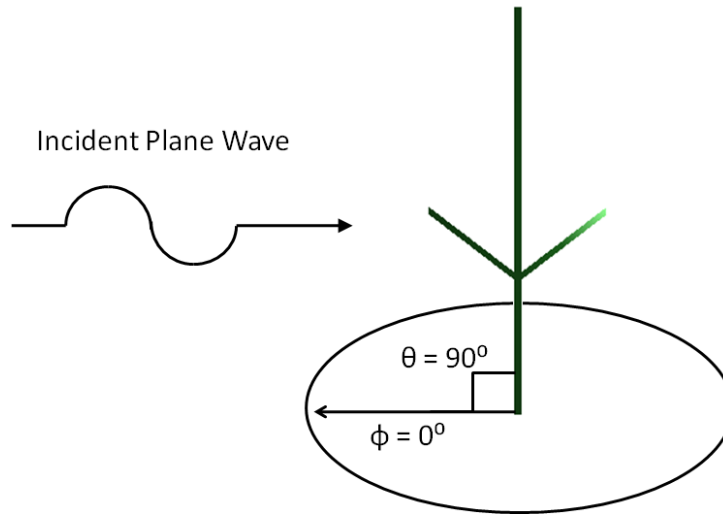


Figure 3.5: Incident Plane Wave Referenced to the Model

resembles a monopole antenna with branches and foliage. This analogous geometry of a pine seedling to a wire antenna is exercised when choosing the analysis tool. For this research the antenna analysis software NEC Win-Pro² is used to simulate a pine seedling model's backscatter. NEC is typically used to simulate wire antennas but will be used for this research to simulate a wire structure resembling a pine seedling. The transmitted power from a radar is modeled in NEC as an incident plane wave [16]. Although a radar's signal originates from a localized antenna, it can be modeled as a plane wave in the far field. NEC uses a polar coordinate system to relate the orientation of the models, the incident plane wave, and the resulting backscatter. The incident plane wave or the transmitted radar signal will originate from a phi angle of zero degrees and a theta angle of ninety degrees as shown in Figure 3.5. The seedling models are suspended in free space and ground parameters are ignored for this experiment.

²Numerical Electromagnetics Code (NEC) uses Method of Moments Analysis (MoM)

Model Geometry

The model's geometry is important since a pine seedling's structure differs for each species of pine. The Loblolly pine seedling structure was selected for one of the geometries for this experiment. The Loblolly pine seedling ideally consist of a central stem with two branches that project from the body at an acute angle. The branches commonly grow out from each row to maximize the amount of sun light absorbed by the foliage. The optimum structure for a Loblolly pine seedling as pictured left in Figure 3.6. Most of the pine seedlings examined in nursery beds resemble the seedling on the right side of the image in Figure 3.6. The shape of a pine seedling is determined from its genetics and the environment. All pine seedlings have a central stem that runs vertically from the root base to the top of the seedling. This commonality among seedlings will be exploited by vertically polarizing the simulated radar signal to couple with a pine seedling's stem [17].

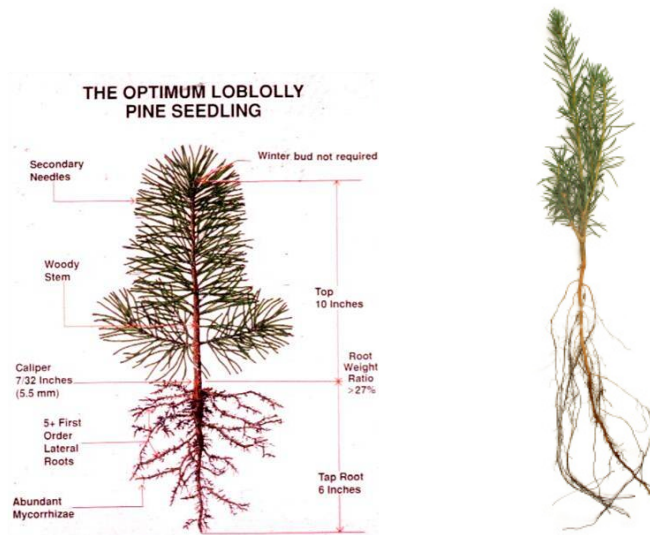


Figure 3.6: Ideal Loblolly Pine & Sample Pine Seedling [21]

Three pine seedling models were developed in the NEC Win-Pro software (Appendix C). Two of the models mimic the geometry of the optimum Loblolly and the sample seedling shown in Figure 3.6. A third branch free NEC model was also included as a structure similar to a monopole antenna for comparison. The pine seedling's needles will not be modeled

because of their mainly horizontal orientation and their small size. The pine needles are not viewed as major contributors to the vertically polarized backscatter. The branches will need to be modeled because of their similarity to both the stem structure and orientation. All three model geometries are shown in Figure 3.7.

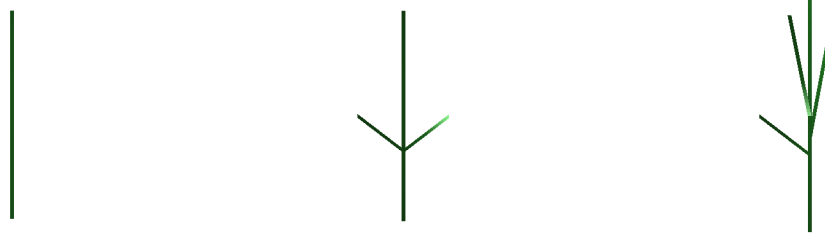


Figure 3.7: NEC Win-Pro Wire Models

Frequency

According to Ikrath [19], trees can be used as monopole antennas for radios. It is known that monopole antennas have a resonant frequency equal to the half wavelength of the antenna. This type of half wavelength resonance is a common principle of operation for monopole antennas. The stem of the pine seedling will then conceivably experience peak resonance when the half wavelength of the radar's carrier frequency is equal to the height of the pine seedling's stem. It is proposed that any additional return produced by branches will be negligible due to the peak resonance of the central stem. This experiment will test the concept of using a half wavelength carrier frequency to generate stem dependent radar return.

Loading

The wire models were loaded under the hypothesis that a loaded antenna is a more accurate model of a pine seedling. They are, by nature, insulators and have been shown to have dynamic resistance and reactance with respect to frequency [7]. Sample pine seedlings have not been measured for their dielectric characteristics. Instead, a broad grouping of

loads common to living pine trees is selected based on Ranson [9] and Sugimoto [10]. Ranson measured Siberian and White pine’s dielectric properties at C-band which is approximately 5 GHz. The work from Sugimoto [10] determined dielectric properties of Hinoki wood from 20 Hz to 10 GHz. Both studies used the complex form of electrical permittivity to measure the wood’s dielectric constant. Both studies show the real permittivity ϵ' to be 2 to 4 times larger than the complex loading ϵ'' . Equation 3.1 gives the notation for a complex dielectric constant.

$$\hat{\epsilon}_r = \epsilon'_r - j\epsilon''_r \tag{3.1}$$

Figure 3.8 graphically illustrates the complex permittivity range of White and Siberian pines recorded in [9]. Five sample dielectric values were selected from the graph to provide a broad range of loadings for each of the pine seedling models. The NEC software tool allows for the seedling models to be loaded as homogeneous structures with each of the five dielectric sample values for each simulation.

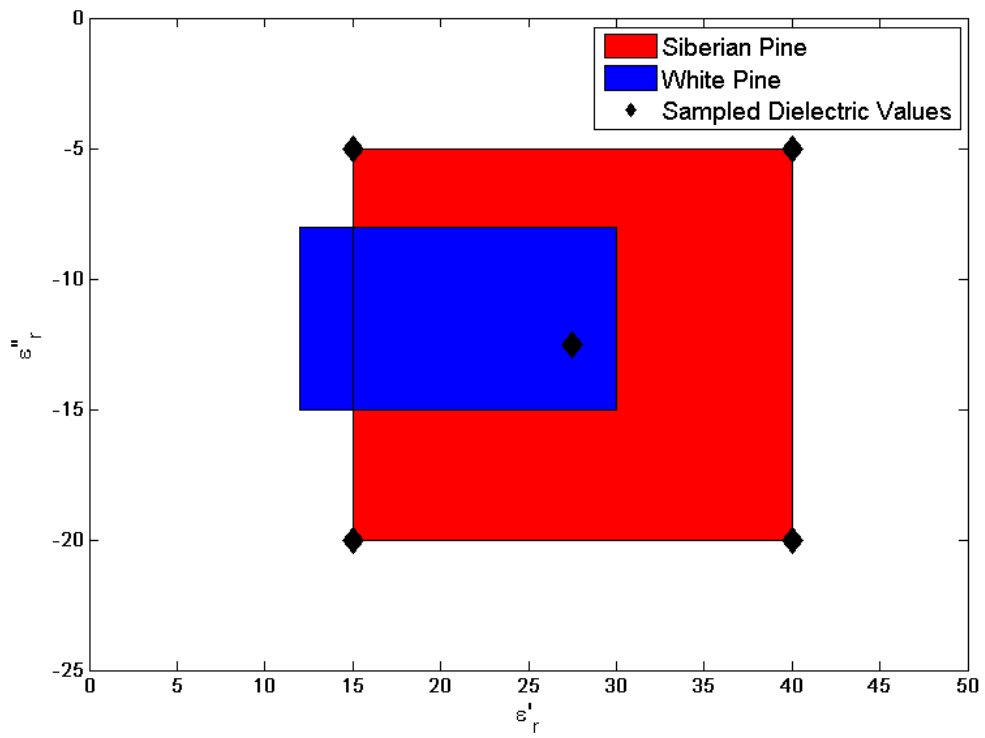


Figure 3.8: Sampled Dielectric Loads

CHAPTER 4

RESULTS AND DISCUSSION

4.1 Photo-Interrupt Results

One of the benefits of the photo-interrupt sensor's configuration was its narrow and tall aperture to help distinguish between stems and horizontal branches. However, experimentation revealed the photo-interrupt sensor to be unable to distinguish between stems and large vertically positioned branches. Lowering the sensor's height to the base of the seedling's stem where the probability of dense foliage was lower caused false interrupts to occur with low branches. Four runs were conducted with the photo-interrupt sensor at different heights from the ground. The results of the experiments are shown in Table 4.1 and indicate false interrupts occur at all heights. The false interrupts caused at 8 centimeters are generated mainly by dense foliage. False interrupts occurring below 8 centimeters were generated primarily by thick vertically oriented branches. The sensor performed well when it was positioned at a height of 6 centimeters, because the foliage was not too dense and the lower branches were not too large to cause an interrupt. The conclusions from this experiment coincided with the study performed in [1].

Height (cm)	Count	Percent Error
2	25	47
4	23	35
6	20	18
8	40	135

Table 4.1: Photo Interrupt Test Results

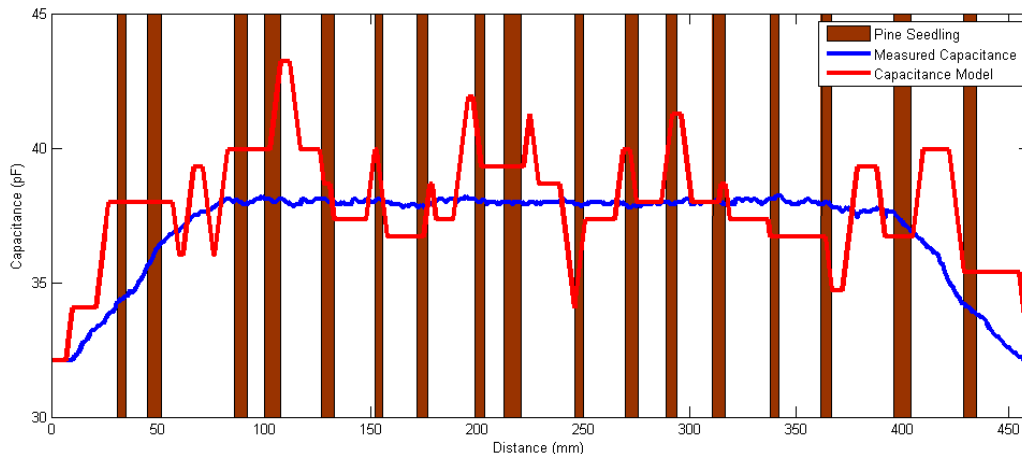


Figure 4.1: Seedling Position and Measured and Modeled Capacitance

4.2 Capacitance Sensor Results

The expectations of the capacitive sensor experiment were that a correlation could be detected between capacitance of the two electrodes and the number of seedlings in their electric field. During experimentation the capacitance of the electrodes changed as individual seedlings passed between the electrodes verifying that pine seedlings are detectable. The capacitance measurement of an individual seedling was recorded and used to generate a model of the sensors output across the artificial test-bed. The model was coded with the assumption that the capacitance of a seedling is based on the amount of stem between the electrodes. The sensor’s model and output from the test bed are graphed in Figure 4.2. The model code and the sensor’s output data are located in appendices D and E respectively.

The capacitive sensor’s output is flat across the artificial test-bed revealing that two seedlings between the electrodes do not add linearly. Furthermore, the sensor offered no distinction between seedlings as they consecutively passed through the electrodes. A second experiment was constructed to test the contribution of foliage to the measured capacitance. The results, Table E, revealed the capacitance of a seedling to be a function of foliage not stem thickness.

4.3 Computer Vision Results

Infrared Spectrum

Pine seedlings were shown to be reflectors of infrared light during a nursery visit in the fall of 2008. An image was retrieved from a guidance camera mounted on the rear of a seedling harvester shown in Figure 4.2. The image is rotated clockwise and the pine seedling stems, bright broad lines, appear slanted left.



Figure 4.2: Seedling Harvester Infra-Red Guidance Camera

The images taken from the experiment are shown in Figure 4.3. They were taken with the Sony Handycam set in IR mode. The images taken with the Handycam match the intensity of the nursery guidance camera image and reaffirm that pine seedlings are good reflectors of infrared light. However, all color information was immediately lost when processing images in infra-red. The remaining image was gray scale measure of the intensity of the reflected infrared light. The pine seedling's intensity was uniform over the entire seedling preventing any distinction between the seedling's stem and the surrounding foliage.

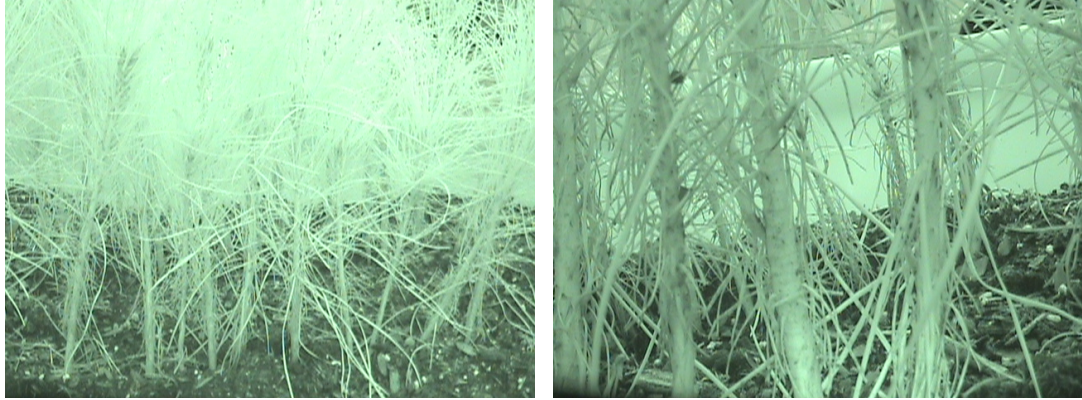


Figure 4.3: Infra-Red Photographs of Artificially Spaced Pine Seedlings

Ultraviolet Spectrum

The ultraviolet spectrum has been known to show fluorescence in certain plants. The ultraviolet spectrum was analyzed using Wood's glass as a lens to filter out the visible spectrum from entering the camera's aperture. The remaining reflected light entering the camera is ultraviolet. Figure 4.4 shows two images taken by the Sony Handycam with a Wood's glass lens. The images reveal no distinction between the pine seedling stems and their foliage.

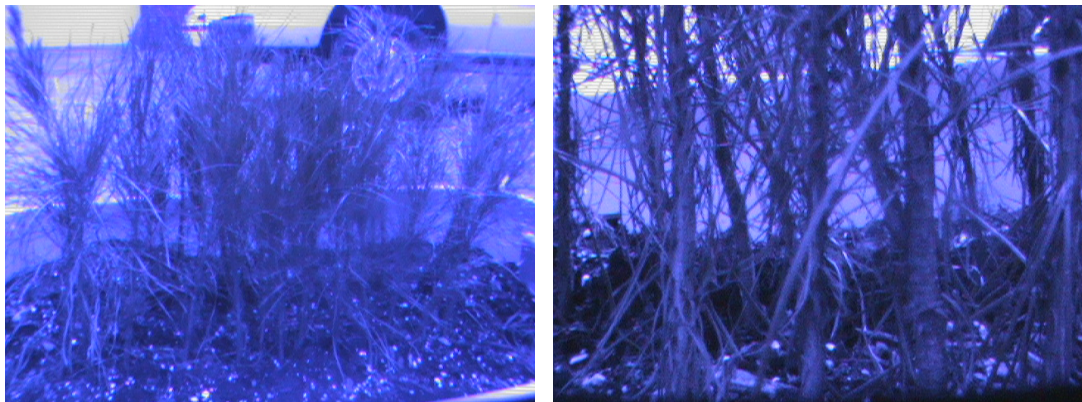


Figure 4.4: Ultra-Violet Photographs of Artificially Spaced Pine Seedlings

Visible Spectrum

In the visible spectrum images are divided into three channels: red, green and blue. Each of these channels is represented by a two-dimensional pixel matrix. Each value in the matrix corresponds to the intensity of the channel's color at that particular pixel location. The visible spectrum has obvious color advantages for distinguishing between stems and foliage. The stems reflect brown light while the foliage typically reflects green light. Figure 4.5 shows light absorption for chlorophyll, a key color component of seedling foliage.

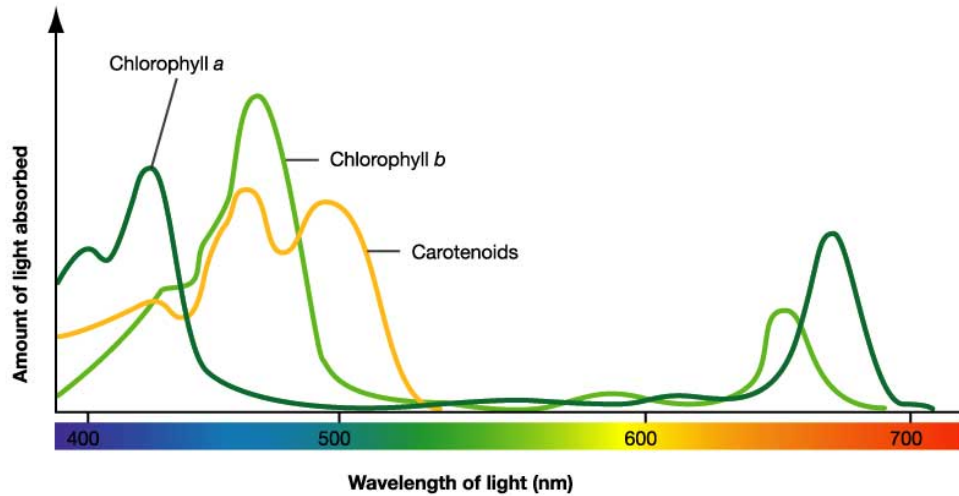


Figure 4.5: Plant Absorption of Light in the Visible Spectrum [14]

The visible spectrum experiment was developed to capitalize on the color distinction between stem and foliage in the visible spectrum. A simple statistical algorithm was developed using the light absorption information from Figure 4.5. MATLAB code was developed to run the algorithm and process the image (Appendix F). The algorithm determines pixel columns that contain a higher concentration of the color brown. These columns should correlate with vertically oriented brown seedling stems. Following equation 4.1, each of the channel's columns, n , were summed and normalized creating a vector for each channel \hat{C}_n .

The vectors \hat{R} , \hat{G} , and \hat{B} represent the average color intensity across the image. The three resulting vectors were weighted, based on the light absorption chart, and added together to form equation 4.2. The remaining vector \hat{D} shows where high concentrations of brown pixels existed in the image.

$$\hat{C}_n = \frac{\sum_1^n C_{m,n}}{m} \quad (4.1)$$

Figure 4.6 is an image of a pine seedling row from a nursery visit. The red, green, and blue lines plotted across the image represent the vectors \hat{R} , \hat{G} , and \hat{B} respectively. The white line represents the calculated vector \hat{D} . The calculated vector equation is based on the color properties of a seedling stem. The results of the algorithm show the vector peaking at locations where seedlings were present. The peaks were obscured by a dynamic threshold across the entire image. Some of the peaks were also obscured by noise in the image. The noise is introduced by the presence of a white shirt sleeve and foliage in the background. The color white especially affects the noise floor because white shares equal parts of high intensity color from each channel. The experiment for the visible spectrum considered that the accuracy of the system could be improved by placing a black background behind the seedling row. Figure 4.7 contains four images from the test-bed with the data vector plotted across each image. The simple algorithm indicates that individual seedlings can be detected in the artificial test-bed.

$$\hat{D} = 2\hat{R} - \hat{G} + 2\hat{B} \quad (4.2)$$

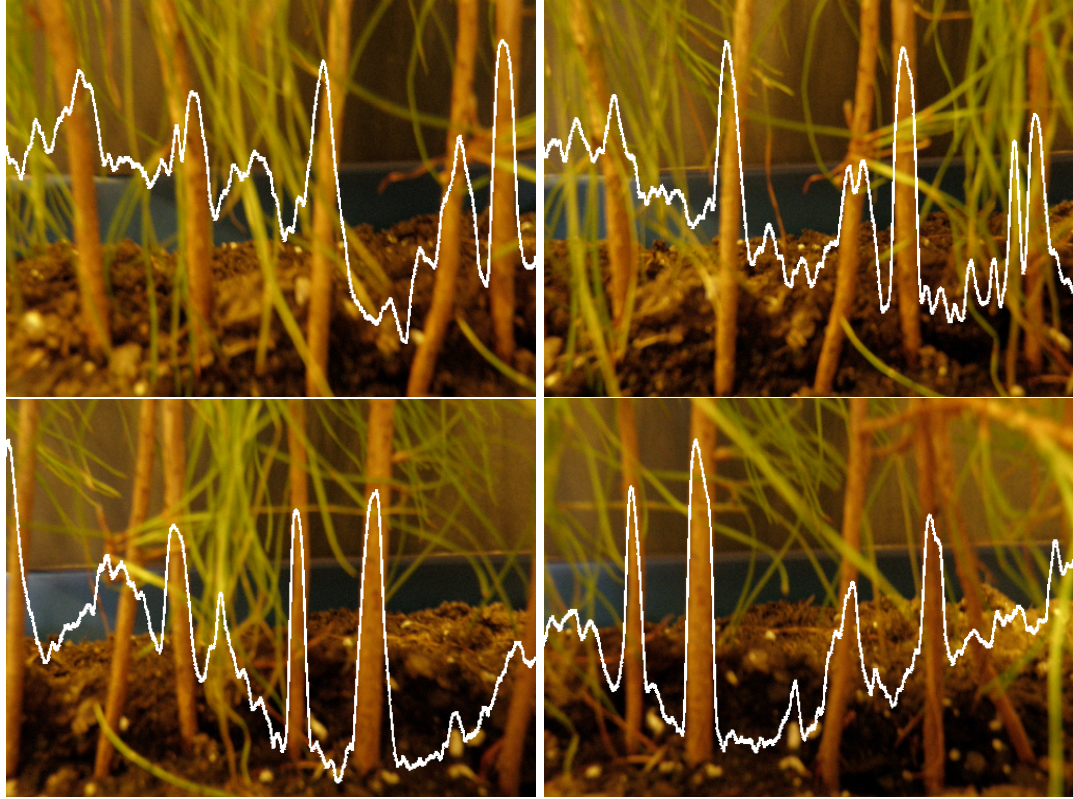


Figure 4.7: Series of Images with Data Vector

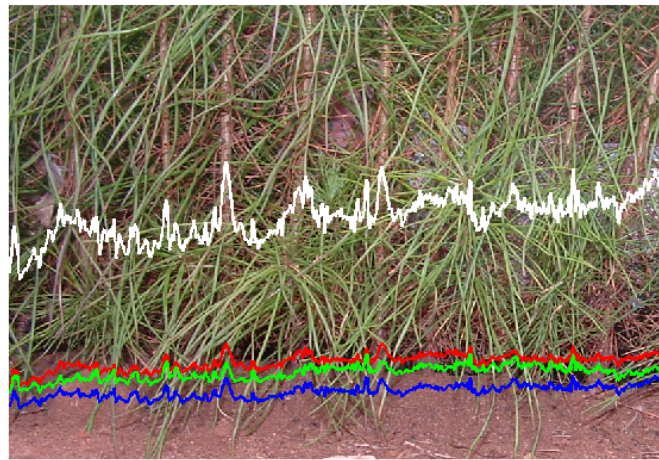


Figure 4.6: Visible Spectrum Analysis

4.4 Radar Results

Radar Return Results

Figure 4.8 shows the results of the first radar experiment from a Tektronics oscilloscope display. The top graph is a control and shows the noise floor. The control was measured from the Pearson coil when it was de-coupled from the seedling. The bottom graph is the signal generated through the seedling by the propagating wideband signal. The signal was measured from the Pearson coil coupled around the base of the seedling. Both measurements were made during a transmission of a wideband pulse. The signal generated by the seedling is shown to be well above the noise floor and is considered detectable by radar.

Radar Backscatter Measurement

The pine seedling models are simulated with a carrier frequency wavelength of $0.14\text{ m} < \lambda_f < 3\text{ m}$, where the pine seedling stem height corresponds to a wavelength $\lambda_P = 0.3\text{ m}$ and is the average height of a pine seedling stem. Sweeping the simulation frequency will make any resonance obvious when analyzing the radar's return. The wavelength is normalized $\lambda = \frac{\lambda_P}{\lambda_f}$, also making the pine seedling wavelength with respect to the frequency wavelength more easily observable. The stem is expected to resonate at the half wavelength frequency and generate a similar return for all three models. A similar radar return for each model will enable the branch geometry to be neglected, making individual pine seedlings realizable by a radar system.

4.4.1 Monopole Tree Model

Figure 4.9 shows the magnitude of the backscatter spreading away from the monopole seedling model at the half wavelength frequency. The plot verifies the expected uniform backscatter for a monopole antenna.

Figure 4.10 is a magnitude plot of the returned backscatter with respect to frequency and loading of the monopole seedling model. The plot represents the radar return from each

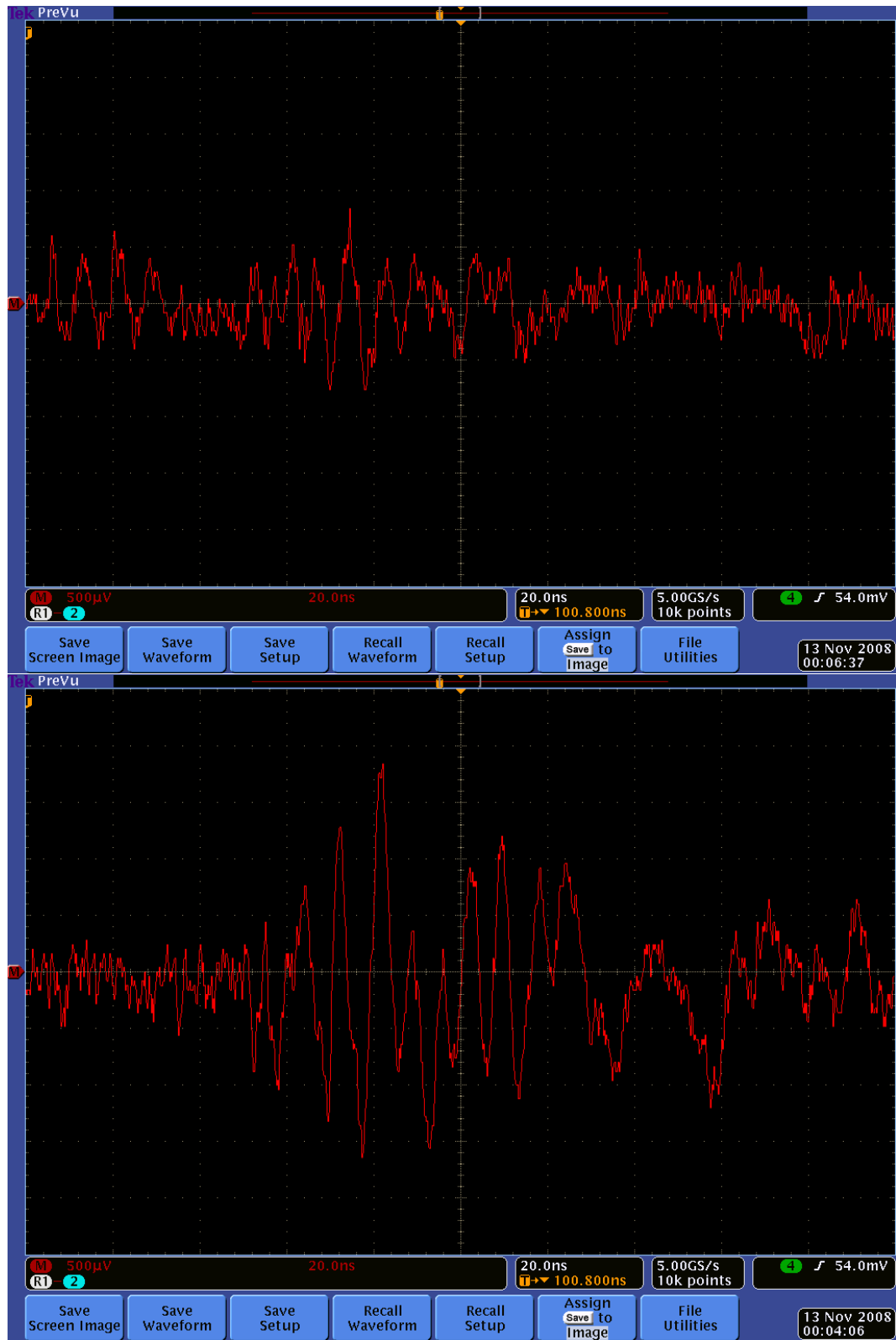


Figure 4.8: Voltage Waveform Induced from the Current Flow through a Pine Seedling due to the presence of an Electromagnetic Field

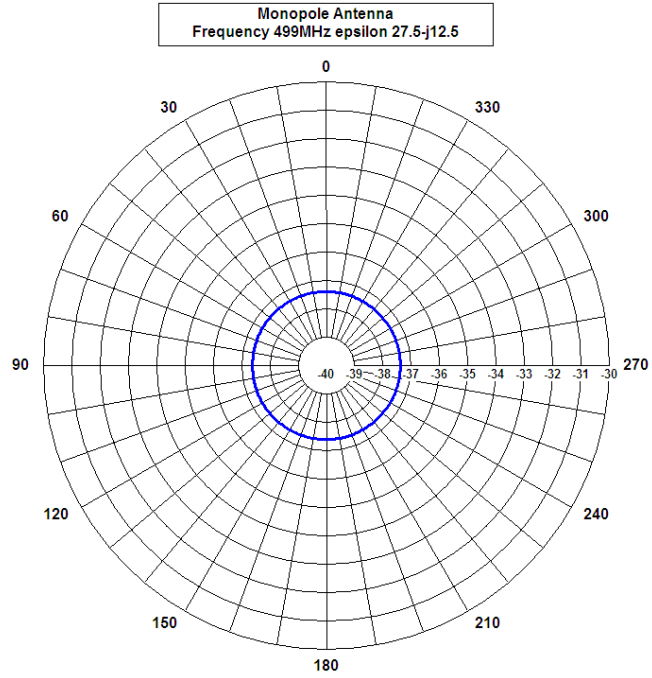


Figure 4.9: Radiation Pattern of the Monopole Tree Model

of the five dielectric loadings. The results show an exponentially decaying increase in the re-radiated power. The expected spike or increase at the resonant frequency is not present for any of the model's dielectric loads.

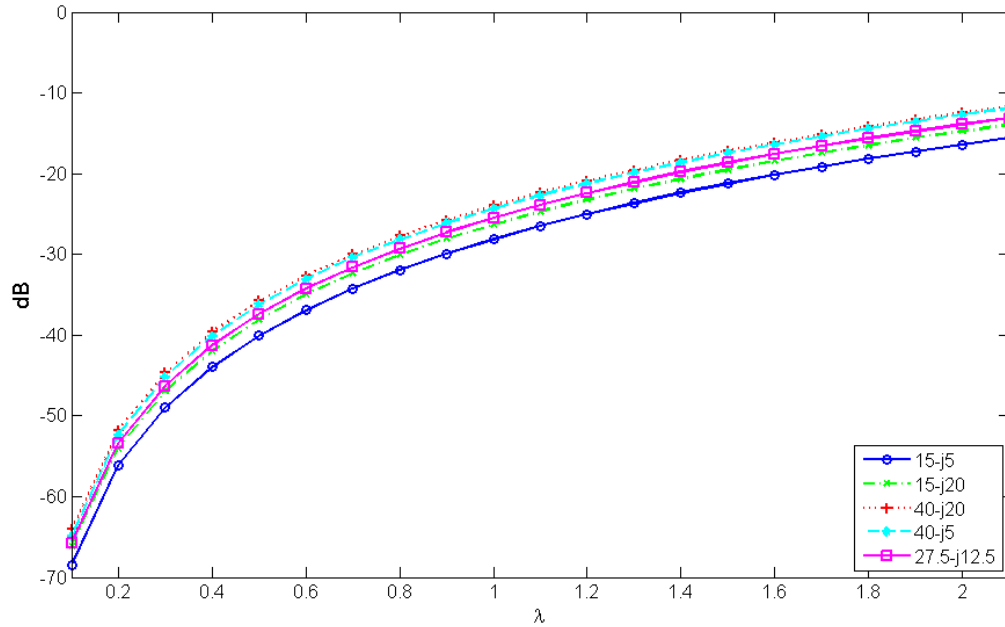


Figure 4.10: Monopole Antenna Reradiated Power

4.4.2 Ideal Loblolly Model

The Loblolly model adds two branches to the previously simulated monopole model. The branches are oriented almost completely on the horizontal axis and are expected to contribute little to the return. Figure 4.11 is a polar plot of the Loblolly model's backscatter at the half wavelength frequency. The backscatter plot shows a slight manipulation to the uniform return observed by the monopole model.

Figure 4.12 plots the returned backscatter with respect to frequency and dielectric loading of the Loblolly model. The results do not show resonance at the half wavelength frequency, but the magnitudes almost perfectly match the monopole seedling model.

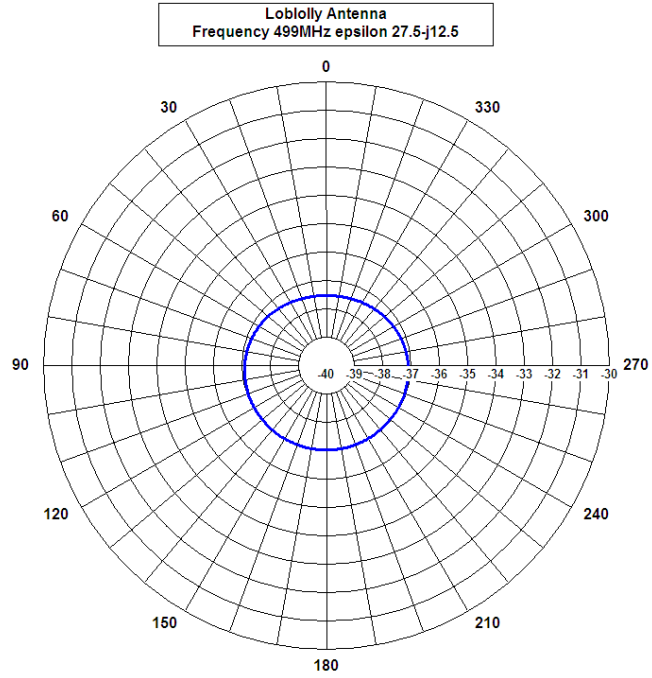


Figure 4.11: Radiation Pattern of Ideal Loblolly Model

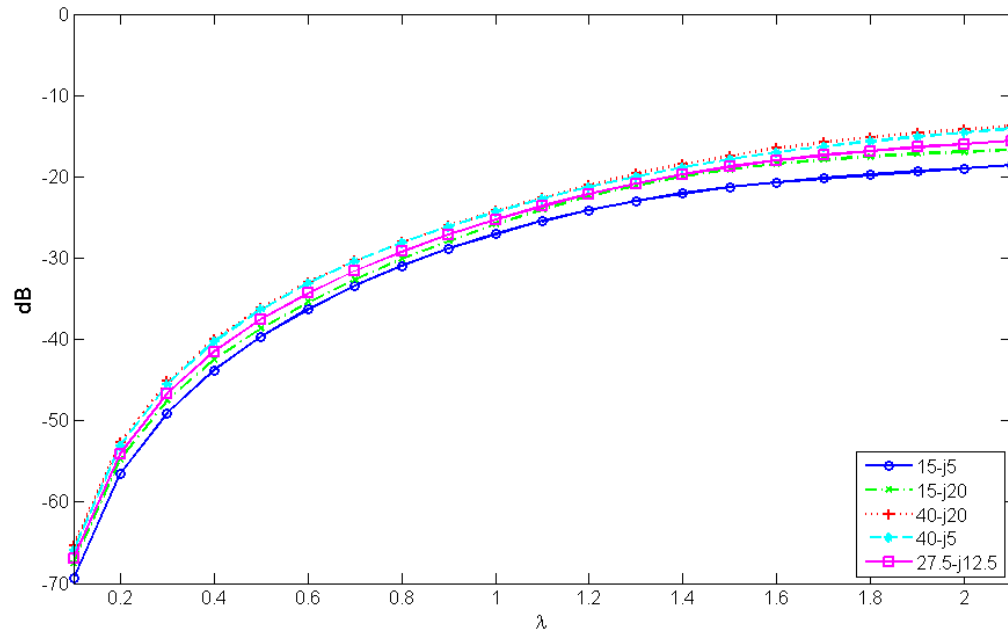


Figure 4.12: Loblolly Antenna Re-radiated Power

4.4.3 Sample Seedling Model

The sample seedling model adds several branches to the monopole model. The branches are positioned more vertically than the previous Loblolly model. The return of the seedling model's stem is expected to be the main contributor to the backscatter and the branches are expected to be negligible. Figure 4.13 is the radar backscatter of the sample seedling model at the half wavelength frequency. The magnitude of the backscatter is almost uniform like the Loblolly and monopoles models, but the magnitude is greater than both models by about 4.5dB.

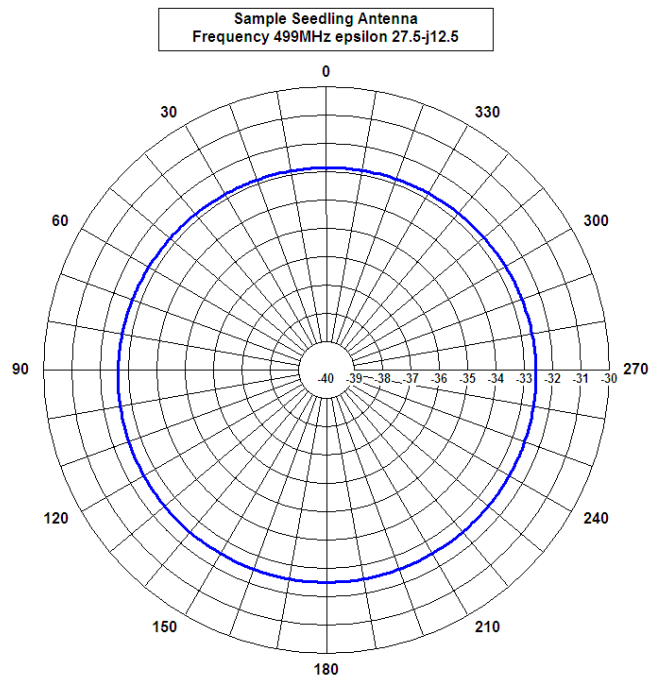


Figure 4.13: Radiation Pattern of the Sample Seedling Model

Figure 4.14 confirms that there is an increase in the amplitude across all measured frequencies. The sample seedling model's return averages to about 3-4 decibels higher when compared to the monopole and Loblolly models over the same frequency span.

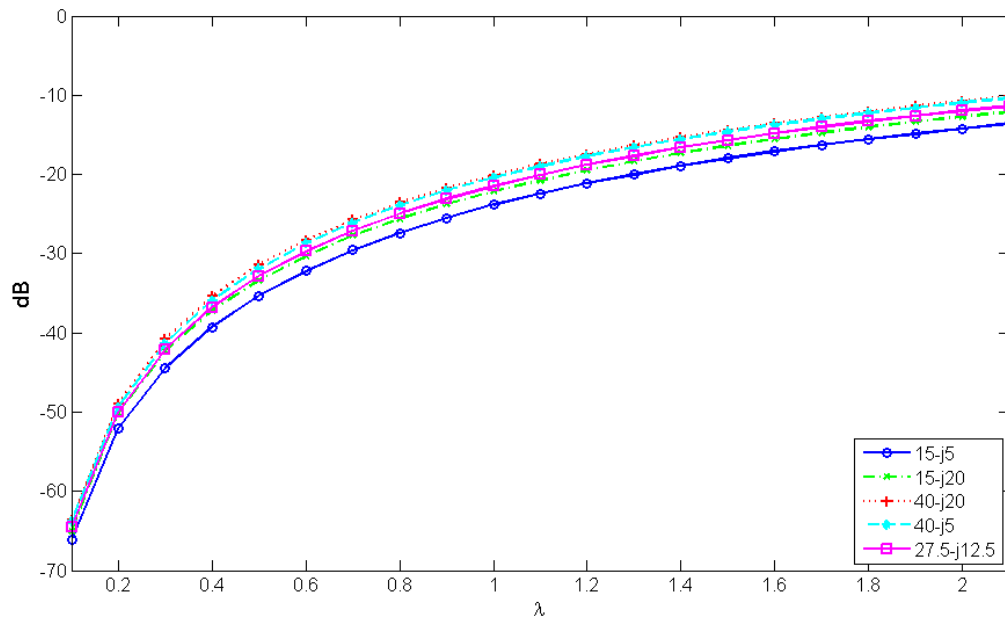


Figure 4.14: Sample Seedling Antenna Re-radiated Power

The results of the models demonstrate that vertically positioned limbs will significantly contribute to radar return. The seedling models did not show any resonance at the half wavelength frequency. The results demonstrate that individual seedlings cannot be determined from radar return at the half wavelength frequency of the seedling's stem.

CHAPTER 5
SUMMARY AND CONCLUSIONS

5.1 Introduction

The goal of this research was to propose a pine seedling detection and registration method for the development of an auto-indexing pine seedling counter. Previous research and literature on the problem was initially reviewed. Two prior studies were found, a patent and a study performed by the USDA forestry service. The patent and study both used photo-interrupts as the method for detection. This thesis identified four sensing technologies and determined their strengths and weaknesses as a pine seedling detection and registration method. Each technology has been tested for its ability to detect a pine seedling.

The results indicated photo-interrupt and capacitive sensing to be poor choices for accurate pine seedling detection. The photo-interrupt system cannot account for false interrupts that can occur in a nursery's environment. Thick foliage and vertically positioned branches were a couple of the nursery conditions identified as a primary causes for false interrupts. The capacitive sensor measures a pine seedling's dielectric constant which is a function of foliage. The foliage of a seedling varies significantly making detection of individual seedlings in a row impossible. Computer vision is a better choice for pine seedling identification. The results of the computer vision experiment demonstrated an accurate indication of a pine seedling's location. However, a computer vision system would experience problems in the tight spaces between rows in a nursery bed. In addition most of the natural sunlight will be blocked by foliage between rows making color distinction very difficult. The nursery's environment would also be harsh on a camera sensor's lens along with the high computational cost that is associated with the large amounts of data a camera collects. A camera system has to detect and register each pine seedling individually in a two dimensional data set. This

system could create an immense processing cost in a nursery consisting of millions of pine seedlings. CW radar was shown to generate a radar return, however simulation did not reveal a resonant frequency for the modeled seedling. CW radar has the potential ability to map a large area of seedlings very quickly. CW radar can also potentially retrieve seedling properties that are not optically detectable such as moisture content which is proportional to the seedling's permittivity and mass.

	Strengths	Weaknesses
Photo-Interrupt	Simple and dependable Easy to count and ensure spacing Maintain size parameters	Subject to nursery environment Cannot distinguish stems from thick foliage or vertical limbs
Capacitive	Robust and low cost	Poor resolution between seedlings Foliage dependent instead of stem
Computer Vision	Object recognition and tracking Color differentiation between stem and foliage	High computational cost Tracking in foliage and nursery environment Needs artificial lighting
Radar	Collect data over a large area	High computational cost High frequency operation for good resolution

Table 5.1: Sensor Strengths and Weaknesses

Objective 1

This research identified five major fundamental sensing methods used in modern inventory control and management. The sensing methods were analyzed and adapted for the detection of pine seedlings. The methods were applied to the problem of pine seedling detection and registration based on their detection capabilities. The method for pine seedling detection was then suggested as experiment parameters.

	Photo-Interrupt	Capacitive	Computer Vision	CW Radar
Impervious to nursery environment	no	yes	no	yes
Inventory during various stages of seedling growth cycle	yes	no	yes	no
On-the-fly operation	yes	yes	yes	yes
Harvester mountable	yes	yes	yes	no
Determine seedlings location (2-D plot)	yes	no	yes	-
None Invasive	yes	yes	yes	yes
Grading capability (RCD)	-	no	yes	-
Identify diseased seedlings	no	no	yes	-

Table 5.2: System Requirements vs. Sensor Capabilities

Objective 2

Four of the five fundamental sensing methods were selected for further testing. The technologies were developed into an experiment to test their ability to detect pine seedlings. The experiments used an artificial pine seedling nursery row as a test bed. The technologies were modeled and analyzed in software when physical experiments were not feasible to test.

Objective 3

Each detection and registration method was analyzed as it pertained to the future development of automated pine seedling detection and registration. The sensing technology's strengths and weaknesses were cataloged in Table 5.1. The sensing methods were then compared to the ideal sensing system in Table 5.2.

5.2 Future Work

The ultimate goal for pine seedling detection and registration is to develop a high resolution detection and mapping system for pine seedlings in the nursery bed. The resolution of the system would need to be accurate down to one centimeter for mapping purposes and

down to one millimeter for sizing and grading. Computer vision meets the most requirements for pine seedling detection and registration system and is logical choice for further development.

Ultra-wideband (UWB) radar is a relatively new technology and was not tested in this thesis. However UWB could conceivably be used to image the stem and branch structure of a group of seedlings using a computed tomography approach. The system would be a millimeter wave version of the InSAR system developed in [5]. The development of an ultra-wideband system would require a more realistic model. For high frequency analysis the foliage would need to be included along with accurate dielectric measurements for different species of pine seedlings. The use of L-system and OpenGL is suggested to grow pine seedlings of a particular species virtually and model them three-dimensionally. The ability to accurately grow a species of pine seedling in software will enable the radar simulation of an entire nursery bed. The radar could then be extensively tested prior to prototyping.

BIBLIOGRAPHY

- [1] Gasvoda, Dave and Herzberg, Diane. "Seedling Counter Field Tests". *Tree Planters' Notes* 44(1):8-12; 1993.
- [2] Nix, Steve. "Nursery Bed of Pine Seedlings". About.com. June 17, 2009. <<http://z.about.com/d/forestry/1/0/F/B/treesrus2.jpg>>
- [3] Rath, Karl Friedrich. "Apparatus for Harvesting and Bundling Plants". United States Patent 4037666. July 26, 1977
- [4] Weyerhaeuser.com. April 23, 2009. <<http://www.weyerhaeuser.com/Businesses>>
- [5] D. W. Liu, Y. Du, G. Q. Sun, W. Z. Yan, and B.-I. Wu. "Analysis of InSAR Sensitivity to Forest Structure Based on Radar Scattering Model." *Progress In Electromagnetics Research, PIER* 84, 149–171, 2008
- [6] Baxtor, Larry. *Capacitive Sensors: Design and Applications*. John Wiley and Sons. 1996
- [7] Yamamoto, Y.; Harada, H.; Yasuhara, K.; Nakamura, T.; Instrumentation and Measurement, *IEEE Transactions on* Volume 44, Issue 3, June 1995 Page(s):729 - 732
- [8] Trabelsi, S.; Nelson, S.O.; Ramahi, O.; *Microwave Conference, 2006. 36th European* 10-15 Sept. 2006 Page(s):447 - 450
- [9] Ranson, K.J.; Rock, B.N.; Salas, W.A.; Smith, K.; Williams, D.L.; *Geoscience and Remote Sensing Symposium, 1992. IGARSS '92. International Volume 2, 1992* Page(s):1283 - 1285
- [10] Sugimoto, Hiroyuki.; Takazawa, Ryosuke.; Norimoto, Misato.; *Dielectric Relaxation Due to Heterogeneous Structure in Moist Wood. Journal of Wood Science, Volume 51, Number 6 / December, 2005*
- [12] Rafael C. Gonzalez and Richard E. Woods. *Digital Image Processing Third Edition*. Upper Saddle River, New Jersey: Pearson Prentice Hall, 2008
- [14] "absorption-spectrum". [wikispaces.com](http://eapbiofield.wikispaces.com/Chapter+10+Review+Macon?f=print). June 20, 2009. <<https://eapbiofield.wikispaces.com/Chapter+10+Review+Macon?f=print>>
- [14] Kumhala, Frantisek.; Prosek, Vaclav.; Kroulik, Milan.; Kviz, Zdenek.; *Parallel Plate Mass Flow Sensor for Forage Crops and Sugar Beet. ASABE Annual International Meeting. 2008 Providence, Rhode Island, June 29 - July 2, 2008* 084700.

- [15] Currie, Nicholas C. Techniques of Radar Reflectivity Measurement. Dedham, MA. Artech House, Inc. 1984.
- [16] Nittany Scientific, Inc. NEC-Win Pro User's Manual. Riverton, UT. 1997
- [17] Skolnik, Merrill I. Introduction to Radar Systems. New York. 1980
- [18] Banner Sensors website. July 3, 2009. <<http://www.bannerengineering.com/en-US/>>
- [19] Ikrath, K.; Kennebeck, W.; Hoverter, R.; Antennas and Propagation, IEEE Transactions on. Volume 23, Issue 1, Jan 1975 Page(s):137-140
- [20] Boyer, James N. and South, David B.. "Loblolly Pine Seedling Morphology and Production at 53 Southern Forest Nurseries". Tree Planters' Notes 39(3):13-16; 1988.
- [21] South, David B.;VanderSchaaf, Curtis L.; "RCDlob". <<http://www.afrc.uamont.edu/vanderschaaf/rcdlob.htm>>

APPENDICES

APPENDIX A

PHOTO-INTERRUPT MICROCONTROLLER SCHEMATIC

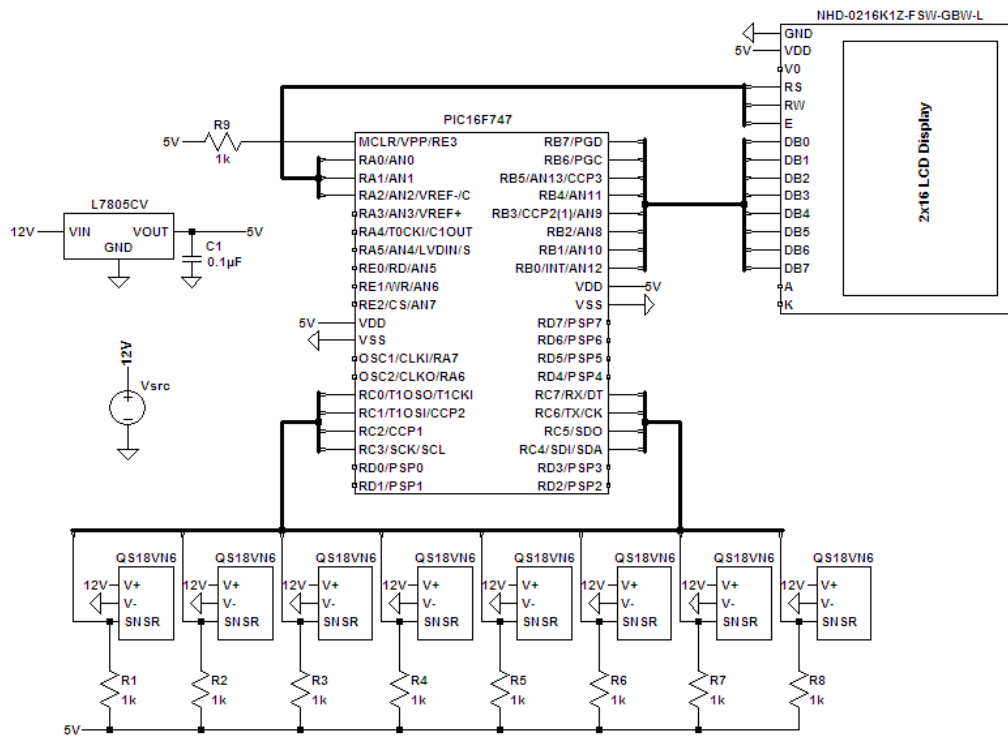


Figure A.1: Photo-Interrupt Microcontroller Schematic

APPENDIX B
PHOTO-INTERRUPT MICROCONTROLLER CODE

```
.*****  
,  
; This file is assembly code for eight binary sensors. Each I/O pin  
; contribute to the over all count. There is approximately 0.5 ms  
; between the checking of each sensors status. Each sensor must  
; must signal a detection and a non-detection to be counted. This  
; limits the number of detections made by one to sensor to 100 per  
; minute.  
.*****  
,  
; Filename: TreeCounter.asm  
; Date: December 2007  
; File Version: 1.0  
; Author: Jeff Hunt  
; Company: Auburn University  
.*****  
,  
; Files required: p16F747.inc  
.*****  
,  
; Notes: This software was developed for the detection of an eight  
; sensor network that could count eight rows of seedlings at once.  
.*****  
,  
#include <p16F747.inc> ; Processor Include file, for standard names  
    CBLOCK 0x20  
ASCII TEMP FLAG  
W_TEMP  
STATUS_TEMP  
SENSORS  
SENSORSF  
SENSOR_0  
SENSOR_1  
SENSOR_2
```



```

SENSOR_3
SENSOR_4
SENSOR_5
SENSOR_6
SENSOR_7
ONES
TENS
HUND
THOU
TTHO
HTHO
MILL
TMIL
CARR
    ENDC
;Start Code
ORG 0 ; Start of code (location 0)
GOTO SETUP
ORG 0X04
GOTO ISR
    SETUP
BANKSEL OSCCON
MOVLW B'01101000'
MOVWF OSCCON
BANKSEL ADCON1
MOVLW 0x0F ;set all A/D pins to Digital I/O
MOVWF ADCON1
BANKSEL TRISC ; BANK 1
MOVLW B'11111111' ; RC7-RC0 are inputs for PORTC
MOVWF TRISC
CLRF TRISB ; all PORTB pins configured for output mode
CLRF TRISA ; all output
;*****MAIN*****
    MAIN

```

```

CALL LCD_SETUP
CLRF ASCII
CLRF TEMP
CLRF FLAG
CLRF MSD
CLRF LSD
CLRF SENSORSF
CLRF CARR
MOVLW 0X30
MOVWF ONES
MOVWF TENS
MOVWF HUND
MOVWF THOU
MOVWF TTHO
MOVWF HTHO
MOVWF MILL
MOVWF TMIL
    MAIN_LOOP
; CALL CHECK_SENSORS
; CALL UPDATE_DISPLAY
GOTO MAIN_LOOP
    CHECK_SENSORS
BANKSEL PORTC
MOVF PORTC,W
MOVWF SENSORS
BTFSS SENSORS,0
GOTO $+3
BCF SENSORSF,0
CLRF SENSOR_0
BTFSC SENSORSF,0
GOTO $+6
INCF SENSOR_0,f
BTFSS SENSOR_0,3
GOTO $+3

```

BSF SENSORSF,0
GOTO UPDATE_COUNT
BTFSS SENSORS,1
GOTO \$+3
BCF SENSORSF,1
CLRF SENSOR_1
BTFSC SENSORSF,1
GOTO \$+6
INCF SENSOR_1,f
BTFSS SENSOR_1,3
GOTO \$+3
BSF SENSORSF,1
GOTO UPDATE_COUNT
BTFSS SENSORS,2
GOTO \$+3
BCF SENSORSF,2
CLRF SENSOR_2
BTFSC SENSORSF,2
GOTO \$+6
INCF SENSOR_2,f
BTFSS SENSOR_2,3
GOTO \$+3
BSF SENSORSF,2
GOTO UPDATE_COUNT
BTFSS SENSORS,3
GOTO \$+3
BCF SENSORSF,3
CLRF SENSOR_3
BTFSC SENSORSF,3
GOTO \$+6
INCF SENSOR_3,f
BTFSS SENSOR_3,3
GOTO \$+3
BSF SENSORSF,3

GOTO UPDATE_COUNT
BTFSS SENSORS,4
GOTO \$+3
BCF SENSORSF,4
CLRF SENSOR_4
BTFSC SENSORSF,4
GOTO \$+6
INCF SENSOR_4,f
BTFSS SENSOR_4,3
GOTO \$+3
BSF SENSORSF,4
GOTO UPDATE_COUNT
BTFSS SENSORS,5
GOTO \$+3
BCF SENSORSF,5
CLRF SENSOR_5
BTFSC SENSORSF,5
GOTO \$+6
INCF SENSOR_5,f
BTFSS SENSOR_5,3
GOTO \$+3
BSF SENSORSF,5
GOTO UPDATE_COUNT
BTFSS SENSORS,6
GOTO \$+3
BCF SENSORSF,6
CLRF SENSOR_6
BTFSC SENSORSF,6
GOTO \$+6
INCF SENSOR_6,f
BTFSS SENSOR_6,3
GOTO \$+3
BSF SENSORSF,6
GOTO UPDATE_COUNT

```

BTFSS SENSORS,7
GOTO $+3
BCF SENSORSF,7
CLRF SENSOR_7
BTFSC SENSORSF,7
GOTO $+6
INCF SENSOR_7,f
BTFSS SENSOR_7,3
GOTO $+3
BSF SENSORSF,7
GOTO UPDATE_COUNT
RETURN
    UPDATE_COUNT
MOVLW 0x06
MOVWF CARR
INCF ONES,f
MOVF ONES,0
ADDWF CARR,1
BTFSS CARR,6
RETURN
MOVLW 0X30
MOVWF ONES
MOVLW 0x06
MOVWF CARR
INCF TENS,f
MOVF TENS,0
ADDWF CARR,1
BTFSS CARR,6
RETURN
MOVLW 0X30
MOVWF TENS
MOVLW 0x06
MOVWF CARR
INCF HUND,f

```

```
MOVF HUND,0
ADDWF CARR,1
BTFSS CARR,6
RETURN
MOVLW 0X30
MOVWF HUND
MOVLW 0x06
MOVWF CARR
INCF THOU,f
MOVF THOU,0
ADDWF CARR,1
BTFSS CARR,6
RETURN
MOVLW 0X30
MOVWF THOU
MOVLW 0x06
MOVWF CARR
INCF TTHO,f
MOVF TTHO,0
ADDWF CARR,1
BTFSS CARR,6
RETURN
MOVLW 0X30
MOVWF TTHO
MOVLW 0x06
MOVWF CARR
INCF HTHO,f
MOVF HTHO,0
ADDWF CARR,1
BTFSS CARR,6
RETURN
MOVLW 0X30
MOVWF HTHO
MOVLW 0x06
```

```

MOVWF CARR
INCF MILL,f
MOVF MILL,0
ADDWF CARR,1
BTFSS CARR,6
RETURN
MOVLW 0X30
MOVWF MILL
MOVLW 0x06
MOVWF CARR
INCF TMIL,f
MOVF TMIL,0
ADDWF CARR,1
BTFSS CARR,6
RETURN
GOTO MESSAGE_1
    UPDATE_DISPLAY
MOVLW 0X40
CALL LCD_COMMAND
MOVF TMIL,0
CALL DISPLAY
MOVF MILL,0
CALL DISPLAY
MOVF HTHO,0
CALL DISPLAY
MOVF TTHO,0
CALL DISPLAY
MOVF THOU,0
CALL DISPLAY
MOVF HUND,0
CALL DISPLAY
MOVF TENS,0
CALL DISPLAY
MOVF ONES,0

```

```

CALL DISPLAY
RETURN
MESSAGE_1
RETURN
.*****END MAIN*****
,
.*****
,
.*****LCD DISPLAY SUBROUTINES*****
,
.*****

    DISPLAY
CALL LCDWAIT
MOVWF PORTB
BSF PORTA,0
BCF PORTA,1 ;R/W is cleared.
BSF PORTA,2
NOP
NOP
BCF
PORTA,2
NOP
NOP
BCF PORTA,0
RETURN
;LCD WAIT ROUTINE IT POLES THE MSB OF THE LCD
    LCDWAIT
BANKSEL TRISB
BSF TRISB,7
BANKSEL PORTA
BSF PORTA,1
BCF PORTA,0
NOP
BSF PORTA,2
BSF PORTA,3
CLRWDI
BTFSC PORTB,7

```



```

GOTO $-2
BCF PORTA,3
BCF PORTA,2
BCF PORTA,2
BCF PORTA,1
BANKSEL TRISB
BCF TRISB,7
BANKSEL PORTA
RETURN
;END OF WAIT ROUTINE
.*****LCD SETUP ROUTINES*****
,
.*****
,

    LCD_SETUP
BANKSEL PORTA
BCF PORTA,0 ;CLEARS OUTPUTS TO LCD
BCF PORTA,1
BCF PORTA,2
SLEEP
MOVLW 0X38
MOVWF PORTB
BSF PORTA,2
NOP
NOP
NOP
NOP
BCF PORTA,2
NOP
NOP
NOP
NOP
MOVLW 0X38
MOVWF PORTB
BSF PORTA,2
NOP

```

```

NOP
NOP
NOP
BCF PORTA,2
CALL WAIT
MOVLW 0X38
MOVWF PORTB
BSF PORTA,2
NOP
NOP
NOP
NOP
BCF PORTA,2
;INTIAL SETUP IS COMPLETE THE LCD IS SET FOR 8 BITS AND MAY
  BE POLLED
MOVLW 0X0C ;DISPLAY IS ON CURSOR IS OFF
CALL WAIT
CALL LCD_COMMAND
MOVLW 0X01 ;CLEARS DISPLAY
CALL LCD_COMMAND
MOVLW 0X06 ;ENTRY MODE CURSOR MOVES LEFT TO RIGHT NO
  SCREEN SHIFT
CALL LCD_COMMAND
MOVLW 0X80 ;RETURNS CURSOR TO HOME (TOP LEFT)
CALL LCD_COMMAND
RETURN
;SETUP OF THE LCD PANNEL IS COMPLETE
;GENERIC SUBROUTINE THAT SENDS A COMMAND BYTE TO THE
  LCD
  LCD_COMMAND ;ACTUALLY SENDS COMMAND LINE TO LCD
CALL LCDWAIT ;SETUP BYTE IS IN W
BANKSEL PORTB
MOVWF PORTB ;OUTPUT TO B
BCF PORTA,0
NOP

```

```

BSF PORTA,2 ;SEND INFO
NOP
NOP ;WAIT
NOP
NOP
BCF PORTA,2 ;STOP BYTE
RETURN
,*****END OF COMMAND*****
,*****
;Displays WAR EAGLE
WAR_EAGLE
BANKSEL PORTA
BSF PORTA,3
BANKSEL 0
MOVLW 0X57
CALL DISPLAY
MOVLW 0X41
CALL DISPLAY
MOVLW 0X52
CALL DISPLAY
MOVLW 0x20
CALL DISPLAY
MOVLW 0X45
CALL DISPLAY
MOVLW 0X41
CALL DISPLAY
MOVLW 0X47
CALL DISPLAY
MOVLW 0X4C
CALL DISPLAY
MOVLW 0X45
CALL DISPLAY
RETURN
    WAIT

```

```
BANKSEL 0
BSF T1CON,5
BCF T1CON,4
CLRF TMR1L
CLRF TMR1H
BCF PIR1,0
BSF T1CON,0
BTFSS PIR1,0
GOTO $-2
BCF T1CON,0
RETURN
    ISR
RETFIE
END
```

APPENDIX C CAPACITIVE SENSOR SCHEMATIC

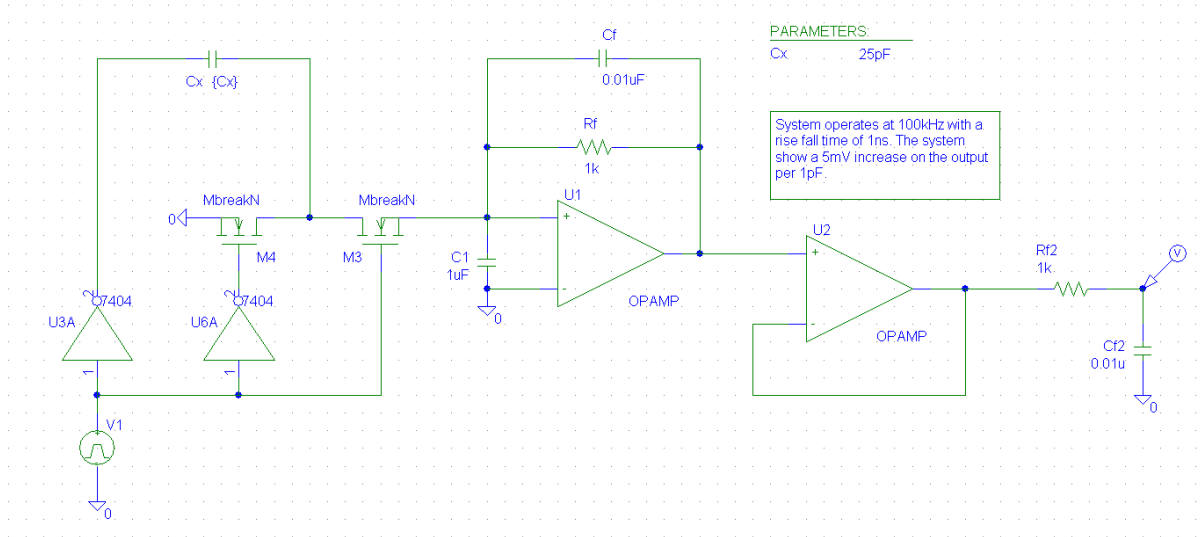


Figure C.1: Capacitive Sensor (C_x represents electrodes)


```

end
% model of over lapping electrode multiplied by the average capacitance per
% mm of seedling plus the base capacitance
model=(model*avgC)+baseC;
C=[32.1,32.1,32.1,32.1,32.1,32.1,32.1,32.1,32.1,32.1,32.3,32.3,32.4,32.6,32.8,32.8...
,32.9,33.1,33.2,33.2,33.3,33.4,33.4,33.5,33.5,33.7,33.8,33.9,33.9,34,34.3,34.3,34.4...
,34.4,34.5,34.5,34.7,34.6,34.7,34.8,35,35.1,35.2,35.4,35.6,35.7,35.8,36,36.2,36.3...
,36.4,36.5,36.5,36.6,36.7,36.8,36.8,36.9,36.9,36.9,37,37.1,37.1,37.3,37.3,37.4,37.5...
,37.5,37.5,37.6,37.6,37.6,37.6,37.7,37.7,37.8,37.8,37.9,37.9,38,38,38.1,38.1,38.1...
,38,38,38.1,38,38,37.9,37.9,37.9,38,38,38,38.1,38.1,38.1,38.2,38.1,38.1,38.1,38.1...
,38,38,38,38.1,38.1,38.1,38,38,37.9,37.9,37.8,37.9,37.9,37.9,38.1,38.1,38,38,38,...
38,38.1,38.1,38.1,38.1,38.1,38.1,38,38,38,38,37.9,37.9,37.9,38,37.9,37.9,37.9...
,37.9,38.1,38.1,38,38,38,38,38.1,38.1,38,38,38,38.1,38.1,38.1,38,38,38,38,37.9...
,37.9,37.9,37.9,37.9,37.8,37.8,37.9,37.8,37.9,37.9,37.9,37.8,37.8,37.9,37.8,37.8...
,37.9,37.9,37.9,38,38,38.1,38.1,38.1,38,38,38.1,38.1,38.1,38,38,38.1,38.1,38.1...
,38.2,38.1,38.1,38.1,38.1,38,38,38,38.1,38,37.9,38,38,38,38,37.9,37.9,38,38,38...
,38,38,37.9,38,38,38,38,37.9,37.9,37.9,38,38,38,37.9,38,37.9,38,38,38,38,38...
,38,38,38,38.1,38.1,38,38,38,38,37.9,37.9,37.9,37.8,37.9,37.9,37.9,38,38,38,38...
,38,38,38,37.9,37.9,37.9,37.9,38,38,37.9,37.9,38,37.9,37.9,37.8,37.8,37.8,37.9...
,37.8,37.9,37.8,37.9,37.9,37.9,37.9,37.9,38,38,37.9,37.9,38,38,38,38,37.9,37.9...
,37.9,38,38,38,38,38.1,38.1,38.1,37.9,37.9,38,38,37.9,38,38,38,38,38,38,38.1...
,38,38,37.9,37.9,37.9,38,37.9,37.9,38.1,38.1,38.1,38,38.1,38.1,38.1,38,38.1,38.1...
,38,38,37.9,38,38,38.1,38.1,38.1,38.1,38.2,38.2,38.2,38.1,38,38,38,37.9,37.9...
,37.9,37.9,38,38,38,38.1,38.1,38,38,38,38,37.9,37.9,37.9,38,38,37.9,37.8,37.8...
,37.8,37.8,37.7,37.6,37.7,37.8,37.7,37.7,37.6,37.6,37.4,37.6,37.6,37.7,37.6,37.6...
,37.6,37.7,37.7,37.7,37.8,37.7,37.6,37.4,37.7,37.6,37.6,37.6,37.5,37.4,37.3,37.3...
,37.1,37.1,37,36.9,36.9,36.8,36.7,36.6,36.6,36.5,36.4,36.3,36.3,36.2,36.1,36.1...
,36,35.7,35.7,35.4,35.2,35,34.9,34.8,34.6,34.5,34.4,34.2,34.2,34.1,34.1,34,33.9...
,33.9,33.8,33.8,33.7,33.7,33.6,33.5,33.3,33.2,33.1,33,33,32.9,32.8,32.7,32.6...
,32.6,32.5,32.4,32.4,32.3,32.2,32.2,32.1,32.2,32.2,32.2];
% Error calculation
SSerr=sum((C-model).^2);
SStot=sum((C-mean(C)).^2);
R=1-(SSerr/SStot);

```

APPENDIX E
CAPACITIVE SENSOR COLLECTED DATA

Seedlings with Foliage (pF)	Seedlings without Foliage (pF)
35.0	32.3
35.1	32.1
34.8	31.8
35.4	31.9
35.1	32.3
35.4	32.3
35.6	32.9
35.3	32.6
35.1	32.5
35.0	32.0
35.2	32.5
35.4	32.3
35.7	32.1
35.3	31.8
35.1	31.8
35.0	32.3
35.2	32.3
35.0	32.4
35.1	32.6
34.8	32.5

Table E.1: Capacitance of Seedlings with and without Foliage

Position (mm)	Root Collar Diameter (mm)
33	3
49	6
81	5
104	7
130	5
154	3
175	4
202	4
217	7
248	3
273	5
292	4
314	5
340	3
365	4
400	7
432	5

Table E.2: Seedling Position and Root Collar Diameter

Distance (mm)	Capacitance (pF)	Model (pF)
1	32.1	32.1
2	32.1	32.1
3	32.1	32.1
4	32.1	32.1
5	32.1	32.1
6	32.1	32.1
7	32.1	32.1
8	32.1	32.8
9	32.1	33.4
10	32.1	34.1
11	32.3	34.1
12	32.3	34.1
13	32.4	34.1
14	32.6	34.1
15	32.8	34.1
16	32.8	34.1
17	32.9	34.1
18	33.1	34.1
19	33.2	34.1
20	33.2	34.1
21	33.3	34.1
22	33.4	34.7
23	33.4	35.4
24	33.5	36.0
25	33.5	36.7
26	33.7	37.3
27	33.8	38.0
28	33.9	38.0
29	33.9	38.0
30	34.0	38.0
31	34.3	38.0
32	34.3	38.0
33	34.4	38.0
34	34.4	38.0
35	34.5	38.0
36	34.5	38.0
37	34.7	38.0
38	34.6	38.0
39	34.7	38.0
40	34.8	38.0
41	35.0	38.0

42	35.1	38.0
43	35.2	38.0
44	35.4	38.0
45	35.6	38.0
46	35.7	38.0
47	35.8	38.0
48	36 .0	38.0
49	36.2	38.0
50	36.3	38.0
51	36.4	38.0
52	36.5	38.0
53	36.5	38.0
54	36.6	38.0
55	36.7	38.0
56	36.8	38.0
57	36.8	38.0
58	36.9	37.3
59	36.9	36.7
60	36.9	36.0
61	37 .0	36.0
62	37.1	36.0
63	37.1	36.7
64	37.3	37.3
65	37.3	38.0
66	37.4	38.6
67	37.5	39.3
68	37.5	39.3
69	37.5	39.3
70	37.6	39.3
71	37.6	39.3
72	37.6	38.6
73	37.6	38.0
74	37.7	37.3
75	37.7	36.7
76	37.8	36.0
77	37.8	36.0
78	37.9	36.7
79	37.9	37.3
80	38 .0	38.0
81	38 .0	38.6
82	38.1	39.3
83	38.1	40.0
84	38.1	40.0

85	38 .0	40.0
86	38 .0	40.0
87	38.1	40.0
88	38 .0	40.0
89	38 .0	40.0
90	37.9	40.0
91	37.9	40.0
92	37.9	40.0
93	38.0	40.0
94	38.0	40.0
95	38.0	40.0
96	38.1	40.0
97	38.1	40.0
98	38.1	40.0
99	38.2	40.0
100	38.1	40.0
101	38.1	40.0
102	38.1	40.0
103	38.1	40.0
104	38.0	40.6
105	38.0	41.3
106	38.0	41.9
107	38.1	42.6
108	38.1	43.2
109	38.1	43.2
110	38.0	43.2
111	38.0	43.2
112	37.9	43.2
113	37.9	42.6
114	37.8	41.9
115	37.9	41.3
116	37.9	40.6
117	37.9	40.0
118	38.1	40.0
119	38.1	40.0
120	38.0	40.0
121	38.0	40.0
122	38.0	40.0
123	38.0	40.0
124	38.1	40.0
125	38.1	40.0
126	38.1	40.0
127	38.1	39.3

128	38.1	38.6
129	38.1	38.6
130	38.0	38.6
131	38.0	38.6
132	38.0	38.0
133	38.0	37.3
134	37.9	37.3
135	37.9	37.3
136	37.9	37.3
137	38.0	37.3
138	37.9	37.3
139	37.9	37.3
140	37.9	37.3
141	37.9	37.3
142	38.1	37.3
143	38.1	37.3
144	38.0	37.3
145	38.0	37.3
146	38.0	37.3
147	38.0	37.3
148	38.1	37.3
149	38.1	38.0
150	38.0	38.6
151	38.0	39.3
152	38.0	40.0
153	38.1	40.0
154	38.1	39.3
155	38.1	38.6
156	38.0	38.0
157	38.0	37.3
158	38.0	36.7
159	38.0	36.7
160	37.9	36.7
161	37.9	36.7
162	37.9	36.7
163	37.9	36.7
164	37.9	36.7
165	37.8	36.7
166	37.8	36.7
167	37.9	36.7
168	37.9	36.7
169	37.9	36.7
170	37.9	36.7

171	37.9	36.7
172	37.8	36.7
173	37.8	36.7
174	37.9	36.7
175	37.8	36.7
176	37.8	37.3
177	37.9	38.0
178	37.9	38.6
179	37.9	38.6
180	38.0	38.0
181	38.0	37.3
182	38.1	37.3
183	38.1	37.3
184	38.1	37.3
185	38.0	37.3
186	38.0	37.3
187	38.1	37.3
188	38.1	37.3
189	38.1	37.3
190	38.0	38.0
191	38.0	38.6
192	38.1	39.3
193	38.1	40.0
194	38.1	40.6
195	38.2	41.3
196	38.1	41.9
197	38.1	41.9
198	38.1	41.9
199	38.1	41.3
200	38.0	40.6
201	38.0	40.0
202	38.0	39.3
203	38.1	39.3
204	38.0	39.3
205	37.9	39.3
206	38.0	39.3
207	38.0	39.3
208	38.0	39.3
209	38.0	39.3
210	37.9	39.3
211	37.9	39.3
212	38.0	39.3
213	38.0	39.3

214	38.0	39.3
215	38.0	39.3
216	38.0	39.3
217	37.9	39.3
218	38.0	39.3
219	38.0	39.3
220	38.0	39.3
221	38.0	39.3
222	37.9	39.3
223	37.9	40.0
224	37.9	40.6
225	38.0	41.3
226	38.0	40.6
227	38.0	40.0
228	37.9	39.3
229	38.0	38.6
230	37.9	38.6
231	38.0	38.6
232	38.0	38.6
233	38.0	38.6
234	38.0	38.6
235	38.0	38.6
236	38.0	38.6
237	38.0	38.6
238	38.0	38.6
239	38.0	38.6
240	38.1	38.0
241	38.1	37.3
242	38.0	36.7
243	38.0	36.0
244	38.0	35.4
245	38.0	34.7
246	37.9	34.1
247	37.9	34.7
248	37.9	35.4
249	37.8	36.0
250	37.9	36.7
251	37.9	37.3
252	37.9	37.3
253	38.0	37.3
254	38.0	37.3
255	38.0	37.3
256	38.0	37.3

257	38.0	37.3
258	38.0	37.3
259	38.0	37.3
260	37.9	37.3
261	37.9	37.3
262	37.9	37.3
263	37.9	37.3
264	38.0	37.3
265	38.0	37.3
266	37.9	38.0
267	37.9	38.6
268	38.0	39.3
269	37.9	40.0
270	37.9	40.0
271	37.8	40.0
272	37.8	40.0
273	37.8	39.3
274	37.9	38.6
275	37.8	38.0
276	37.9	38.0
277	37.8	38.0
278	37.9	38.0
279	37.9	38.0
280	37.9	38.0
281	37.9	38.0
282	37.9	38.0
283	38.0	38.0
284	38.0	38.0
285	37.9	38.0
286	37.9	38.0
287	38.0	38.0
288	38.0	38.6
289	38.0	39.3
290	38.0	40.0
291	37.9	40.6
292	37.9	41.3
293	37.9	41.3
294	38.0	41.3
295	38.0	41.3
296	38.0	41.3
297	38.0	40.6
298	38.1	40.0
299	38.1	39.3

300	38.1	38.6
301	37.9	38.0
302	37.9	38.0
303	38.0	38.0
304	38.0	38.0
305	37.9	38.0
306	38.0	38.0
307	38.0	38.0
308	38.0	38.0
309	38.0	38.0
310	38.0	38.0
311	38.0	38.0
312	38.0	38.0
313	38.1	38.0
314	38.0	38.0
315	38.0	38.6
316	37.9	38.6
317	37.9	38.6
318	37.9	38.0
319	38.0	38.0
320	37.9	37.3
321	37.9	37.3
322	38.1	37.3
323	38.1	37.3
324	38.1	37.3
325	38.0	37.3
326	38.1	37.3
327	38.1	37.3
328	38.1	37.3
329	38.0	37.3
330	38.1	37.3
331	38.1	37.3
332	38.0	37.3
333	38.0	37.3
334	37.9	37.3
335	38.0	37.3
336	38.0	37.3
337	38.1	36.7
338	38.1	36.7
339	38.1	36.7
340	38.1	36.7
341	38.2	36.7
342	38.2	36.7

343	38.2	36.7
344	38.1	36.7
345	38.0	36.7
346	38.0	36.7
347	38.0	36.7
348	37.9	36.7
349	37.9	36.7
350	37.9	36.7
351	37.9	36.7
352	38.0	36.7
353	38.0	36.7
354	38.0	36.7
355	38.1	36.7
356	38.1	36.7
357	38.0	36.7
358	38.0	36.7
359	38.0	36.7
360	38.0	36.7
361	37.9	36.7
362	37.9	36.7
363	37.9	36.7
364	38.0	36.7
365	38.0	36.0
366	37.9	35.4
367	37.8	34.7
368	37.8	34.7
369	37.8	34.7
370	37.8	34.7
371	37.7	34.7
372	37.6	34.7
373	37.7	35.4
374	37.8	36.0
375	37.7	36.7
376	37.7	37.3
377	37.6	38.0
378	37.6	38.6
379	37.4	39.3
380	37.6	39.3
381	37.6	39.3
382	37.7	39.3
383	37.6	39.3
384	37.6	39.3
385	37.6	39.3

386	37.7	39.3
387	37.7	39.3
388	37.7	39.3
389	37.8	38.6
390	37.7	38.0
391	37.6	37.3
392	37.4	36.7
393	37.7	36.7
394	37.6	36.7
395	37.6	36.7
396	37.6	36.7
397	37.5	36.7
398	37.4	36.7
399	37.3	36.7
400	37.3	36.7
401	37.1	36.7
402	37.1	36.7
403	37.0	36.7
404	36.9	36.7
405	36.9	36.7
406	36.8	37.3
407	36.7	38.0
408	36.6	38.6
409	36.6	39.3
410	36.5	40.0
411	36.4	40.0
412	36.3	40.0
413	36.3	40.0
414	36.2	40.0
415	36.1	40.0
416	36.1	40.0
417	36.0	40.0
418	35.7	40.0
419	35.7	40.0
420	35.4	40.0
421	35.2	40.0
422	35.0	40.0
423	34.9	39.3
424	34.8	38.6
425	34.6	38.0
426	34.5	37.3
427	34.4	36.7
428	34.2	36.0

429	34.2	35.4
430	34.1	35.4
431	34.1	35.4
432	34.0	35.4
433	33.9	35.4
434	33.9	35.4
435	33.8	35.4
436	33.8	35.4
437	33.7	35.4
438	33.7	35.4
439	33.6	35.4
440	33.5	35.4
441	33.3	35.4
442	33.2	35.4
443	33.1	35.4
444	33.0	35.4
445	33.0	35.4
446	32.9	35.4
447	32.8	35.4
448	32.7	35.4
449	32.6	35.4
450	32.6	35.4
451	32.5	35.4
452	32.4	35.4
453	32.4	35.4
454	32.3	35.4
455	32.2	35.4
456	32.2	34.7
457	32.1	34.1
458	32.2	33.4
459	32.2	32.8
460	32.2	32.1

Table E.4: Measured and Modeled Capacitance as a Function of Position in the Test Bed

APPENDIX F
MATLAB CODE FOR IMAGE PROCESSING

pic2data.m

```
function [data,R,G,B] = pic2data(pic)
pic = getsnapshot(obj);
[m,n]=size(pic);
R=pic(:,:,1); G=pic(:,:,2); B=pic(:,:,3);
R=sum(R)./m; G=sum(G)./m; B=sum(B)./m;
data=(2*R-G+2*B);
```

treecount.m

```
function treecount
%%%%%%%%%%%%%%%%%%%%%%%%%%%%%%%%%%%%%%%%%%%%%%%%%%%%%%%%%%%%%%%%%%%%%%%%
%initilize webcam
% %%%%%%%%%%%
% Construct a video input object associated
% with a Matrox device at ID 1.
obj = videoinput('matrox', 1);
% Select the source to use for acquisition.
set(obj, 'SelectedSourceName', 'input1')
% View the properties for the selected video source object.
src_obj = getselectedsource(obj);
get(src_obj)
% Preview a stream of image frames. Important because
% webcam shows dark images unless preview is running.
preview(obj);
%%%%%%%%%%%%%%%%%%%%%%%%%%%%%%%%%%%%%%%%%%%%%%%%%%%%%%%%%%%%%%%%%%%%%%%%
%initialize variables%
%%%%%%%%%%%%%%%%%%%%%%%%%%%%%%%%%%%%%%%%%%%%%%%%%%%%%%%%%%%%%%%%%%%%%%%%
master=0; data=0; count=0;
%%%%%%%%%%%%%%%%%%%%%%%%%%%%%%%%%%%%%%%%%%%%%%%%%%%%%%%%%%%%%%%%%%%%%%%%
```

```

%program%
%%%%%%%%%
data=pic2data;
master=trealign(master,data);
[count,master]=counter(master);

```

trealign.m

```

function [data] = trealign(data1,data2)
%assumed that the data is always moving forward!
[row1,column1]=size(data1);
[row2,column2]=size(data2);
shft=0; diff=10;
for n=1:column2;
sub=abs(sum((data1(column1-n+1:column1)-data2(1:n)))/n);
if sub < diff
shft=n; diff=sub;
end
end
if max(data1) > max(data2)
data=[data1,data2(shft:column2)];
else
data=[data1(1:column1-shft),data2];
end
end

```

APPENDIX G
NEC WIN-PRO CODE FOR PINE SEEDLING MODELS

Monopole Antenna

```
CM NEC Input File
CM Monopole radius 0.00275m, length 0.3m
CM excitation by incident plane wave
CE
GW 1 21 0 0 0 0 0.3 0.00275
GS 0 0 1.000000
GE 0
LD 4 1 1 13 871.5 188.7
EX 1 1 1 0 90 0 0 0 0
FR 0 21 0 0 99.930819 99.930819
RP 0 1 360 1000 90 0 1.00000 1.00000
EN
```

Loblolly Antenna Model

```
CM NEC Input File
CM Monopole radius 0.01m, length .3 meters
CM Also wires that resemble seedling
CM limbs will ajoin the monopole (0.002m diameter)
CE
GW 1 21 0 0 0 0 0.30 .00275 !Stem
GW 2 5 0 0 .1 0.05 0 .15 .001 !Branch Right
GW 3 5 0 0 .1 -.05 0 .15 .001 !Branch Left
GS 0 0 1.000000
GE 0
LD 4 1 1 13 871.5 188.7
LD 4 2 1 3 201.1 43.5
LD 4 3 1 5 201.1 43.5
FR 0 21 0 0 99.930819 99.930819
EX 1 1 1 0 90 0 0 0 0
RP 0 1 360 1000 90 0 1.00000 1.00000
EN
```

Sample Seedling Antenna Model

```
CM NEC Input File
CM Monopole radius 0.01m, length .3 meters
CM Also, wires that resemble seedling
CM limbs will ajoin the monopole (0.002m diameter)
CE
GW 1 21 0 0 0 0 0 .30 .00275 !Stem
GW 2 5 0 0 .1 .05 0 .15 .001 !Branch Right
GW 3 9 0 0 .15 .02 .01 .28 .001 !Second Stem
GW 4 10 0 0 .12 -.02 -.01 .26 .001 !Third Stem
GS 0 0 1.000000
GE 0
LD 4 1 1 13 871.5 188.7
LD 4 2 1 5 335.1 72.6
LD 4 3 1 9 603.3 130.6
LD 4 4 1 10 670.3 145.2
FR 0 21 0 0 99.930819 99.930819
EX 1 1 1 0 90 0 0 0 0
RP 0 1 360 1000 90 0 1.00000 1.00000
EN
```


APPENDIX H
SIMULATED RADAR RETURN DATA

Monopole Antenna

Power (dB)	Dielectric Constant $\hat{\epsilon}$				
Frequency (MHz)	15-j5	15-j20	40-j5	40-j20	27.5-j12.5
99.93	-68.48	-66.11	-64.06	-64.84	-65.73
199.86	-56.16	-54.02	-51.81	-52.39	-53.45
299.79	-49.01	-46.95	-44.67	-45.19	-46.30
399.72	-43.97	-41.96	-39.64	-40.12	-41.27
499.65	-40.08	-38.12	-35.78	-36.22	-37.39
599.58	-36.92	-34.99	-32.64	-33.06	-34.24
699.52	-34.25	-32.36	-30.01	-30.4	-31.59
799.45	-31.95	-30.09	-27.73	-28.11	-29.31
899.38	-29.93	-28.09	-25.74	-26.10	-27.30
999.31	-28.13	-26.31	-23.95	-24.30	-25.51
1099.20	-26.50	-24.70	-22.35	-22.68	-23.89
1199.20	-25.02	-23.23	-20.89	-21.21	-22.42
1299.10	-23.66	-21.89	-19.55	-19.86	-21.07
1399.00	-22.40	-20.65	-18.31	-18.62	-19.83
1499.00	-21.24	-19.5	-17.17	-17.46	-18.68
1598.90	-20.15	-18.43	-16.10	-16.39	-17.60
1698.80	-19.13	-17.42	-15.10	-15.38	-16.59
1798.80	-18.18	-16.40	-14.16	-14.44	-15.65
1898.70	-17.26	-15.59	-13.28	-13.54	-14.75
1998.60	-16.40	-14.74	-12.44	-12.70	-13.91
2098.50	-15.59	-13.94	-11.65	-11.90	-13.10

Table H.1: Monopole Antenna Reradiated Power (dB)

Loblolly Antenna Model

Power (dB)	Dielectric Constant $\hat{\epsilon}$				
Frequency (MHz)	15-j5	15-j20	40-j5	40-j20	27.5-j12.5
99.93	-69.39	-67.57	-65.37	-65.93	-66.92
199.86	-56.54	-54.75	-52.63	-53.05	-54.10
299.79	-49.10	-47.52	-45.19	-45.55	-46.68
399.72	-43.81	-42.51	-40.02	-40.30	-41.50
499.65	-39.69	-38.65	-36.10	-36.30	-37.53
599.58	-36.30	-35.44	-32.96	-33.08	-34.31
699.52	-33.43	-32.65	-30.34	-30.40	-31.58
799.45	-30.97	-30.15	-28.08	-28.11	-29.22
899.38	-28.85	-27.89	-26.06	-26.11	-27.12
999.31	-27.02	-25.85	-24.22	-24.32	-25.26
1099.20	-25.45	-24.03	-22.55	-22.72	-23.60
1199.20	-24.12	-22.45	-21.04	-21.29	-22.13
1299.10	-23.00	-21.12	-19.67	-20.00	-20.84
1399.00	-22.07	-20.01	-18.47	-18.87	-19.73
1499.00	-21.31	-19.13	-17.42	-17.87	-18.80
1598.90	-20.69	-18.43	-16.53	-17.01	-18.02
1698.80	-20.18	-17.90	-15.79	-16.28	-17.37
1798.80	-19.75	-17.50	-15.16	-15.64	-16.84
1898.70	-19.37	-17.20	-14.64	-15.08	-16.38
1998.60	-18.99	-16.96	-14.19	-14.58	-15.98
2098.50	-18.56	-16.74	-13.77	-14.09	-15.58

Table H.2: Loblolly Antenna Model Reradiated Power (dB)

Sample Seedling Antenna Model

Power (dB)	Dielectric Constant $\hat{\epsilon}$				
Frequency (MHz)	15-j5	15-j20	40-j5	40-j20	27.5-j12.5
99.93	-66.16	-64.99	-63.66	-63.79	-64.57
199.86	-52.12	-50.12	-48.95	-49.40	-50.05
299.79	-44.47	-42.37	-40.81	-41.35	-42.12
399.72	-39.25	-37.24	-35.41	-35.93	-36.82
499.65	-35.30	-33.36	-31.41	-31.89	-32.85
599.58	-32.17	-30.28	-28.28	-28.70	-29.71
699.52	-29.58	-27.74	-25.71	-26.09	-27.14
799.45	-27.40	-25.60	-23.56	-23.90	-24.97
899.38	-25.53	-23.76	-21.71	-22.03	-22.03
999.31	-23.80	-22.16	-20.11	-20.40	-21.49
1099.20	-22.44	-20.75	-18.70	-18.97	-20.06
1199.20	-21.16	-19.49	-17.44	-17.70	-18.79
1299.10	-20.00	-18.36	-16.31	-16.56	-17.65
1399.00	-18.95	-17.33	-15.30	-15.54	-16.62
1499.00	-17.99	-16.39	-14.37	-14.61	-15.68
1598.90	-17.11	-15.54	-13.53	-13.75	-14.83
1698.80	-16.31	-14.75	-12.75	-12.97	-14.04
1798.80	-15.56	-14.01	-12.03	-12.25	-13.31
1898.70	-14.87	-13.33	-11.36	-11.58	-12.63
1998.60	-14.22	-12.69	-10.74	-10.96	-12.00
2098.50	-13.61	-12.10	-10.15	-10.38	-11.41

Table H.3: Sample Seedling Antenna Model Re-Radiated Power (dB)